

UMTRI-88-5

**THREE-DIMENSIONAL SIMULATION OF OCCUPANT KINEMATICS  
IN ROLLOVERS**

D.H. Robbins

The University of Michigan  
Transportation Research Institute  
Ann Arbor, Michigan 48109-2150

**FINAL REPORT**  
January 1988

Prepared for

Biomedical Science Department  
General Motors Research Laboratories  
Warren, Michigan 48090

Technical Report Documentation Page

1. Report No. UMTRI-88-5		2. Government Accession No.		3. Recipient's Catalog No.	
4. Title and Subtitle  THREE-DIMENSIONAL SIMULATION OF OCCUPANT KINEMATICS IN ROLLOVERS				5. Report Date January 1988	
				6. Performing Organization Code	
7. Author(s) D. H. Robbins				8. Performing Organization Report No. UMTRI-88-5	
9. Performing Organization Name and Address University of Michigan Transportation Research Institute 2901 Baxter Road Ann Arbor, Michigan 48109-2150				10. Work Unit No.	
				11. Contract or Grant No. P.O. #P0000933	
12. Sponsoring Agency Name and Address Biomedical Science Department General Motors Research Laboratories Warren, Michigan 48090				13. Type of Report and Period Covered FINAL REPORT Oct. 1983 - June 1985	
				14. Sponsoring Agency Code	
15. Supplementary Notes					
16. Abstract  This project was a continuation of activity begun with a series of simulations using MVMA 2-D occupant dynamics software. The goals included: (1) full-scale three-dimensional representation of a dolly drop rollover test; (2) comparison between two- and three-dimensional results; (3) inclusion of truly three-dimensional translational and rotational vehicle motions; (4) simulation of two occupants in front seat of vehicle; and (5) development of three-dimensional biomechanically-based neck model. The primary goals of this project were accomplished. The goal of development of a humanlike three-dimensional neck model was postponed until the biomechanical data base defining three-dimensional head motion with respect to the neck was more established.					
17. Key Words  Occupant motion, Crash victim simulation, Rollover accidents			18. Distribution Statement  None		
19. Security Classif. (of this report) None		20. Security Classif. (of this page) None		21. No. of Pages 86	22. Price

# CONTENTS

LIST OF TABLES .....	v
LIST OF FIGURES .....	vi
1.0 INTRODUCTION .....	1
2.0 BACKGROUND AND PROJECT HISTORY .....	2
3.0 PRELIMINARY SIMULATIONS .....	4
3.1 Input Data Set Description .....	4
3.2 Simulation Results .....	6
4.0 FULL-SCALE ROLLOVER SIMULATION .....	15
4.1 Vehicle Description .....	15
4.2 Occupant Description .....	15
4.3 Vehicle Motion .....	33
4.4 Results .....	33
4.5 Conclusions and Recommendations .....	54
5.0 GUIDELINES FOR THE LAYOUT OF GMCVS SEGMENT DATA ...	55
5.1 General Terminology and Definitions .....	55
5.1.1 Segments .....	55
5.1.2 Connections .....	55
5.1.3 Chains and Links .....	55
5.1.4 Branches .....	57
5.1.5 Uniqueness of Paths .....	57
5.1.6 Preferred Order of Segments .....	57
5.1.7 An Unusual Twenty-One Segment Man .....	59
5.2 Description of the CVS Input Data Cards for Segment Definition ..	62
5.2.1 Segment Cards (B.2) .....	62
5.2.2 Joint Cards (B.3-B.5) .....	62
5.2.3 Vehicle Specifications (C.1-C.5) .....	62
5.2.4 Contact Surface Cards (D.2) .....	63
5.2.5 Ellipsoid Cards (D.5) .....	63
5.2.6 Interaction Specifications and Roll Constraints (F.1 and F.3) .....	63
5.2.7 Segment Constraints (D.6) .....	63
5.2.8 Segment Kinematics Output Control Cards (H.1-H.6) .....	63

5.3 Four Related Examples .....	64
5.3.1 Vehicle Crash with Occupant, Column Mass, and Wheel Mass .....	64
5.3.2 Collision of Two Vehicle with Non-Zero Velocities .....	67
5.3.3 Rollover of Vehicle with Two Occupants .....	70
5.3.4 Segment Rolling Over Surface of Another Segment .....	74
<b>6.0 THREE-DIMENSIONAL NECK MODELING CONCEPTS .....</b>	<b>80</b>
<b>7.0 SUMMARY OF RESULTS, CONCLUSIONS,     AND RECOMMENDATIONS .....</b>	<b>83</b>
<b>8.0 REFERENCES .....</b>	<b>85</b>

## LIST OF TABLES

	Page
1. Head/Vehicle Interaction Forces (Simple Rollover) .....	12
2. Chest/Vehicle Interaction Forces (Simple Rollover) .....	12
3. Hip/Vehicle Interaction Forces (Simple Rollover) .....	13
4. Thigh/Vehicle Interaction Forces (Simple Rollover) .....	13
5. Peak Acceleration Exceeding 10 G's for Head (Simple Rollover) .....	14
6. Peak Acceleration Exceeding 10 G's for Torso (Simple Rollover) .....	14
7. Peak Acceleration Exceeding 10 G's for Legs (Simple Rollover) .....	14
8. Full-Scale Simulation Data Set .....	22
9. List of Dummy Segments and Contact Ellipsoids .....	30
10. List of Allowed Occupant Contacts with the Vehicle .....	31
11. Contact Forces Between Occupant and Vehicle .....	37
12. Peak Resultant G-Loadings on Occupant .....	39
13. Order of Segments as a Function of Base Link Choice .....	61
14. B.2 Card Information with NSEG=5 .....	66
15. B.3 Card Information with NJNT=5 .....	66
16. D.2 Card Information with NPL=5 .....	66
17. F.1 Card Information (8 Interactions) .....	66
18. B.2 Card Information with NSEG=12 .....	69
19. B.3 Card Information with NJNT=11 .....	69
20. D.2 Card Information with NPL=12 .....	70
21. F.1 Card Information (18 Interactions) .....	70
22. B.2 Card Information with NSEG=6 .....	73
23. B.3 Card Information with NJNT=6 .....	73
24. D.2 Card Information with NPL=7 .....	74
25. F.3 Card Information (9 Interactions) .....	74
26. F.1 Card Information (37 Interactions) .....	77
27. B.2 Card Information with NSEG=4 .....	78
28. B.3 Card Information with NJNT=3 .....	78
29. D.2 Card Information with NPL=6 .....	78
30. F.3 Card Information (1 Interaction) .....	79
31. F.1 Card Information (10 Interactions) .....	79

## LIST OF FIGURES

	Page
1. Schematic of simple two-vehicle impact with rollover (occupant included) . . . . .	5
2. Simple rollover simulation. Time=0 milliseconds . . . . .	7
3. Simple rollover simulation. Time=100 milliseconds . . . . .	8
4. Simple rollover simulation. Time=200 milliseconds . . . . .	9
5. Simple rollover simulation. Time=1000 milliseconds . . . . .	10
6. Simple rollover simulation. Time=2000 milliseconds . . . . .	11
7. Initial MVMA 2-D configuration of occupant in vehicle for simulation of dolly drop rollover . . . . .	16
8. MVMA 2-D vehicle interior contact surfaces (view from front) . . . . .	17
9. Side view of 3-D occupant in vehicle (Y-Z plane) . . . . .	18
10. Side view of 3-D occupant in vehicle (X-Z plane) . . . . .	19
11. Top view of 3-D occupant in vehicle (X-Y plane) . . . . .	20
12. Occupant contact ellipsoids . . . . .	21
13. Horizontal motion of vehicle . . . . .	34
14. Vertical motion of vehicle . . . . .	35
15. Roll angle of vehicle . . . . .	36
16. Side view of X-Z plane. 0 and 50 milliseconds . . . . .	43
17. Side view of X-Z plane. 100 and 150 milliseconds . . . . .	44
18. Side view of X-Z plane. 200 and 250 milliseconds . . . . .	45
19. Side view of X-Z plane. 300 and 350 milliseconds . . . . .	46
20. Side view of X-Z plane. 400 and 450 milliseconds . . . . .	47
21. Side view of X-Z plane. 500 milliseconds . . . . .	48
22. View from back of Y-Z plane. 0 and 300 milliseconds . . . . .	49
23. View from back of Y-Z plane. 450 milliseconds . . . . .	50
24. Tracing of driver from rear seat camera view. 0 millisecond . . . . .	51
25. Tracing of driver from rear seat camera view. ~250 milliseconds. . . . .	52
26. Tracing of driver from rear seat camera view. ~500 milliseconds . . . . .	53
27. Typical segment . . . . .	56
28. Three branches of three segments each forming one chain of seven segments . . . . .	58
29. An unusual twenty-one segment man . . . . .	60
30. Three-segment man in vehicle with two attached segments . . . . .	65
31. Two three-segment vehicles, with three-segment men inside, collide . . . . .	68
32. Two occupants in vehicle rollover . . . . .	72
33. Rolling segment on pelvis of occupant in vehicle . . . . .	76
34. Humanlike neck model concepts . . . . .	81

## 1.0 INTRODUCTION

The University of Michigan Transportation Research Institute has conducted a study entitled *Three-Dimensional Simulation of Occupant Kinematics in Rollovers*. This work was a continuation of activity begun with a series of simulations using MVMA 2-D occupant dynamics software. The goals were expanded to include: (1) a full-scale three-dimensional representation of the original dolly drop test; (2) a comparison between the two- and three-dimensional results; (3) inclusion of truly three-dimensional translational and rotational vehicle motions; (4) simulation of two occupants in the front seat of the vehicle; and (5) development of a three-dimensional biomechanically based neck model.

The primary goal of this project, development of a rollover simulation capability using three-dimensional crash victim simulation software compatible with that already installed at General Motors, was accomplished. The goal of development of a humanlike three-dimensional neck model was postponed until the biomechanical data base defining three-dimensional head motion with respect to the neck was more established.

Part 2 of this report gives background information and the history of activity on the project. Part 3 presents initial simulation results demonstrating the capability of the General Motors three-dimensional crash victim simulation code (GMCVS) to handle a variety of rollover and impact problems. Part 4 documents the full-scale rollover simulation of the dolly drop test. In Part 5 guidelines are given for the layout of GMCVS segment data. These guidelines include the case of two occupants in the front seat of a vehicle. The preliminary work done to define three-dimensional neck modeling concepts is reported in Part 6. Part 7 is a summary of results, conclusions, and recommendations while Part 8 lists the references.

## 2.0 BACKGROUND AND PROJECT HISTORY

This section of the report discusses the goals of the project and the results that are presented in the report. The initial goals of the project were to:

- Conduct simulation activities on a version of the three-dimensional crash victim simulator compatible with the one installed at General Motors (GMCVS),
- Conduct computer simulations of rollovers to duplicate MVMA 2-D work already accomplished (intrusion, belts, and fifteen-mass occupant),
- Develop three-dimensional biomechanical neck model,
- Include second occupant in the front seat (two occupants, three masses each), and
- Simulate roll with fully three-dimensional vehicle motion components such as a spin followed by a roll.

The first of these goals was to install at UMTRI a version of the Calspan three-dimensional crash victim simulation code compatible with the one in use at General Motors (GMCVS). To accomplish this, the GMCVS, derived from Version 20, was obtained from the Engineering Mechanics Department at General Motors Research Laboratories. It was installed for use on projects sponsored by General Motors requiring three-dimensional crash victim simulation techniques (1,2). A kinematics graphics display package, the "Ellipsoidal Man Plotting Package for MVMA 2-D and CVS (HSRI Version) Occupant Motion Models" (3), was modified for use with GMCVS. This graphics package has already been used with the MVMA 2-D model in the earlier rollover project (4,5). The version used during this project is called GUCVS.

The second of these goals was to duplicate the two-dimensional simulation prepared during the earlier rollover project. Successful completion of several steps was required to reach this goal. The most difficult of these were:

- Simulation of three-dimensional vehicle interior geometry,
- Modeling vehicle motion using the spline-fit algorithm, and
- Coping with extensive computer run time for a problem of this magnitude.

Although time-consuming, simulation of three-dimensional vehicle interior geometry was accomplished without any problems. However, virtually no data were available to describe the deformation characteristics of the various vehicle interior surfaces.

Modeling vehicle motion was a major problem. Many simulation attempts were made before it was determined that the spline-fit software was not working properly. At this point in time, the project had already been in place for one year. It was found that the Aerospace Medical Research Laboratory (AMRL), similarly attempting to simulate rollover and actively working on improvements to the code, was also not satisfied with spline-fit results for duplicating vehicle motions. They provided an improved version of the



code a few months later. Five months, and several additional corrections later, a version of the spline-fit algorithm code was able to process the roll input data set used so easily with the MVMA 2-D code. Thus, after the project had been active for eighteen months, simulation was begun in earnest. Even at this stage, the spline-fit code was very sensitive to initial shape of vehicle motion curves, and to this date requires great care in its use.

The major remaining problem was cost, on the University of Michigan computer system, of the long duration computer runs required to successfully simulate a complete complex rollover event. Complete simulations were conducted for simplified rollovers. However, budget constraints permitted only a partial simulation of the complete event. Input data sets are included in the report for future use.

The third of the goals was development of a three-dimensional biomechanical neck model. The motivation for this was activity of several researchers during the 1983-1984 period. These included:

- Wismans and Spenny (6) who developed representations of head-neck response in frontal flexion
- Bowman et al. (7) who were doing preliminary work on simulations of head motion with respect to the torso
- Alem et al. (8) who were obtaining biomechanical data describing head and neck response to axial impacts
- Goldsmith, Deng, and Merrill (9) who developed a sophisticated three-dimensional head-neck model including effects of individual vertebrae and muscles

In each case, the conclusion was reached that the results were preliminary and that further research was needed. In addition, the biomechanical data base was different for each group, with the exception of the first two, and the human data were obtained at very low G-levels. As a result, little work was done toward this goal because of the very large amount of time that would be required to synthesize the results of the above researchers into a biomechanically sound model and the small range of applicability such a model would have. Several GMCVS modeling concepts have been posed in Section 6 that could be used in future efforts.

The fourth goal was to include a second occupant in the front seat of the vehicle. Preliminary data sets were developed for inclusion of multiple occupants in the vehicle. The description of these data is included in Section 5.

The fifth goal was simulation of a fully three-dimensional rollover such as a spin followed by a roll. During the implementation of properly operating spline-fit code for the description of vehicle motions and accelerations, the function of input to all degrees of freedom of vehicle motion was checked. All appeared to be operating properly.

In conclusion, the primary goal of this project, development of a rollover simulation capability using three-dimensional crash victim simulation software compatible with that already installed at General Motors, was accomplished. The goal of development of a humanlike three-dimensional neck model was postponed until the biomechanical data base defining three-dimensional neck motion was more established.

### 3.0 PRELIMINARY SIMULATIONS

The purpose of this section of the report is to document initial work on the three-dimensional simulation of occupant motions during a rollover. The objective of the work is to demonstrate the capability of the three-dimensional GMCVS code to handle this problem.

The two background documents used in the initiation of this work are by Robbins et al. (10) and Padgaonkar et al. (11). The work by Robbins utilized a fifteen-mass occupant seated in a vehicle subjected to a direct side impact. Side door intrusion was allowed. Padgaonkar used a smaller number of masses (seven) to simulate two impacting vehicles with a three-mass occupant in one of them. The vehicles were each simulated using two masses—a body mass and a bumper mass for both the bullet and target vehicles. A direct side impact was simulated.

The current work expanded on these activities to include rollover and the possibility of interactions such as vehicle-to-vehicle and vehicle-to-ground. The next two sections describe the input data set and the results generated during its exercise.

#### 3.1 INPUT DATA SET DESCRIPTION

Figure 1 is a front-view schematic of the problem that demonstrates a few of the capabilities of the GMCVS software. The two spheres, labeled T and V, are attached to two vehicle masses for sensing contact between the vehicles and with the sloping ground line. Attached to vehicle T is a stylized vehicle interior represented by a six-sided box. The six contact surfaces represent six typical vehicle interior surfaces with which the occupant can interact. A three-mass occupant linkage is positioned within the box. The three masses represent the head, torso, and legs. Attached to the occupant are four ellipsoids to sense contact with the vehicle interior. The head and thigh ellipsoids are attached to the head and leg segments while both the chest and hip are attached to the torso mass. A traditional side view of the occupant and stylized vehicle interior is drawn to the right of the front view in Figure 1.

In order to start the simulation, the vehicle in which the occupant is riding (T) is given an initial translational velocity of 10 miles per hour and a rotational velocity that will yield one complete roll during the simulation time of 2000 milliseconds—a typical time duration for one complete vehicle roll. The vehicle, V, is initially stationary. This idealized problem can be visualized as a case where a vehicle with an occupant is sliding sideways toward a stationary vehicle. Roll is initiated at the moment of contact. The capabilities that are demonstrated by this simulation include:

- Rolling and translating vehicle
- Contact between vehicles
- Three-dimensional occupant in a three-dimensional vehicle
- Ground interactions

It was not necessary to include vehicle contact or ground interactions. These were included only to show the ease with which these types of interactions can be included and to test GMCVS capabilities to simulate multiple linkages simultaneously—a feature

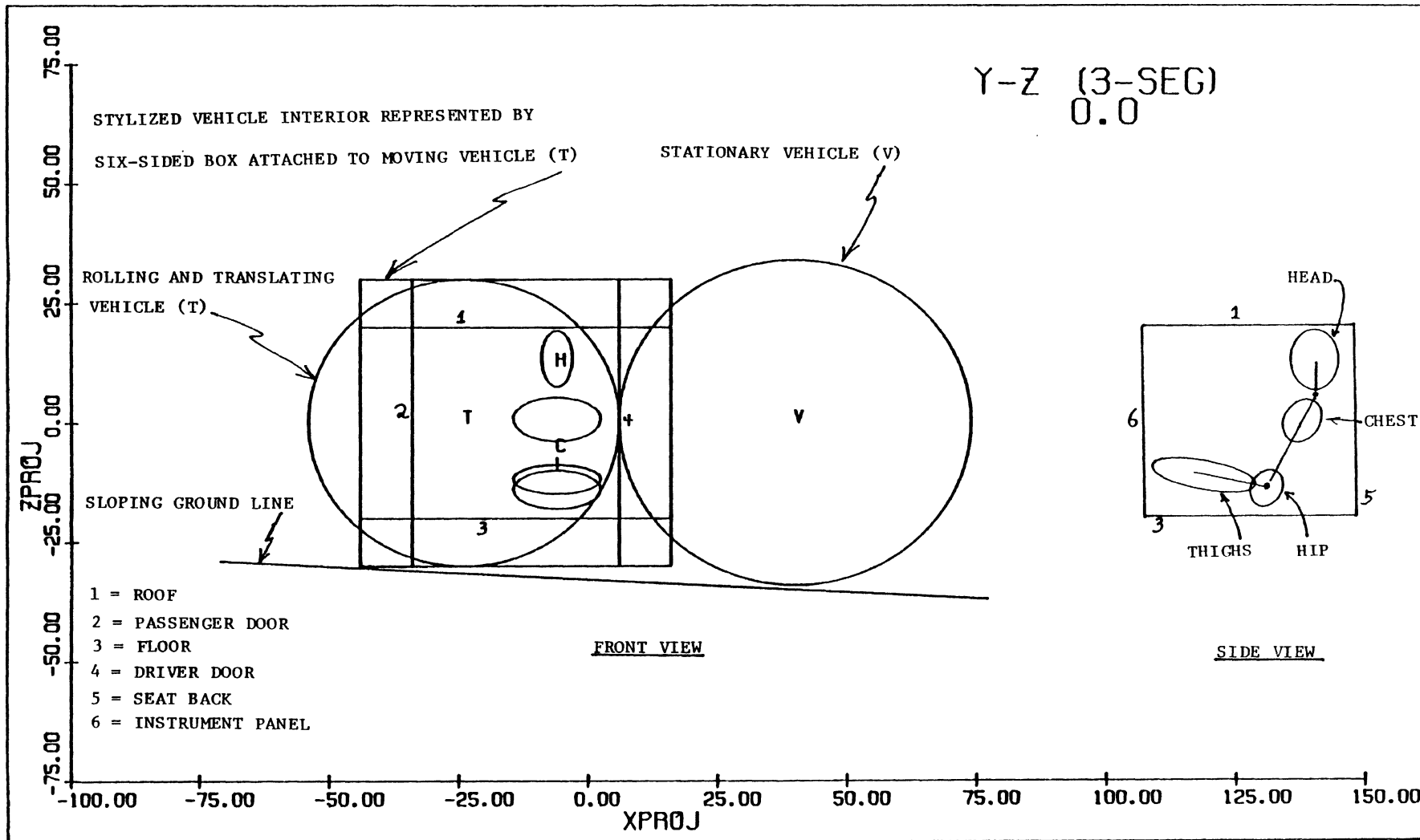


FIGURE 1. Schematic of simple two-vehicle impact with rollover (occupant included).

necessary for multiple occupant simulations. It should be noted that recent reports by Kaleps et al. (12) and Obergefell et al. (13) have reported success in the use of the general vehicle motion input vectors and belt restraints using the HARNESS algorithm.

### 3.2 SIMULATION RESULTS

Five figures and seven tables illustrate the results generated during the 2000-millisecond simulation. Figure 2, at 0 milliseconds, is a repeat of Figure 1 showing the initial position. An "x" has been added to show the change in orientation of the rolling vehicle as a function of time. At 100 milliseconds, (Figure 3), the vehicles are interacting with each other. The slowing of the translating vehicle has caused the occupant to move toward the vehicle side structures. Its rotation has resulted in a contact between the head of the occupant and the roof of the vehicle. By 200 milliseconds, (Figure 4), the vehicles have separated with the translating vehicle now nearly stationary except for rotation. Both vehicles are now interacting with the ground due to the effect of gravity. The occupant has also dropped in relation to the vehicle interior in addition to a variety of interactions. By 1000 milliseconds, (Figure 5), the vehicle is inverted with the occupant pulled around to be in contact with the roof as the vehicle rotates. Because of the interactions between the occupant and the vehicle, the vehicle motions have been slightly altered as shown by the three-dimensional skewing of the occupant compartment lines. By 2000 milliseconds, (Figure 6), the vehicle is again nearly upright. The occupant is likewise nearly in his original configuration.

Tables 1-4 show a summary of the interaction forces between the four occupant ellipsoids and the vehicle. Each table includes the sequence of interactions. The vehicle contact surface, time duration of the contact, and peak force are all included. It should be noted that the head and thigh ellipsoids contact all six of the vehicle surfaces while the torso ellipsoids contact four or more.

Tables 5-7 summarize the resultant G-levels on the three body segments. All peak G-levels larger than 10 are included. The time of the peak is also included as well as any interactions with the vehicle which are taking place at that same time. In some cases, it appears that an interaction between the vehicle and occupant results in increased G's in body segments adjacent to the one that is contacted. These secondary reactions are also noted (in parenthesis).

In summary, the capabilities of the GMCVS have been demonstrated to be applicable to the case of a rollover. Logical extensions of this work include:

- Comparison of MVMA 2-D results already generated with three-dimensional results using a more detailed vehicle configuration including instrument panel, steering column, and steering wheel surfaces
- Inclusion of general translational and rotational components as input data to describe vehicle motion
- Simulation of multiple occupants in a vehicle
- Development of a detailed biomechanical neck model for use in studying head/neck response to contact with the vehicle interior
- Use of restraint systems (belts in particular)

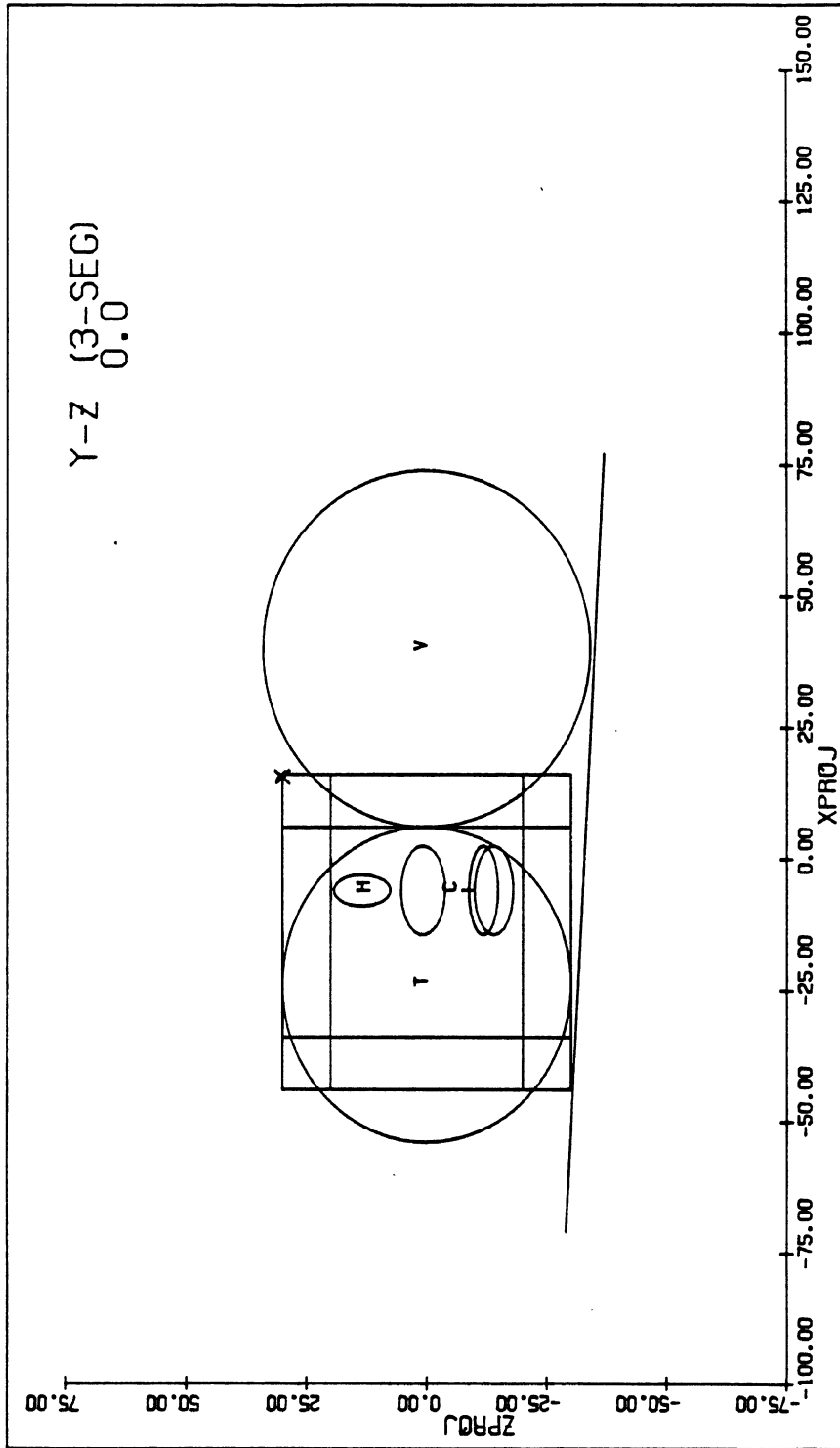


FIGURE 2. Simple rollover simulation. Time = 0 milliseconds.

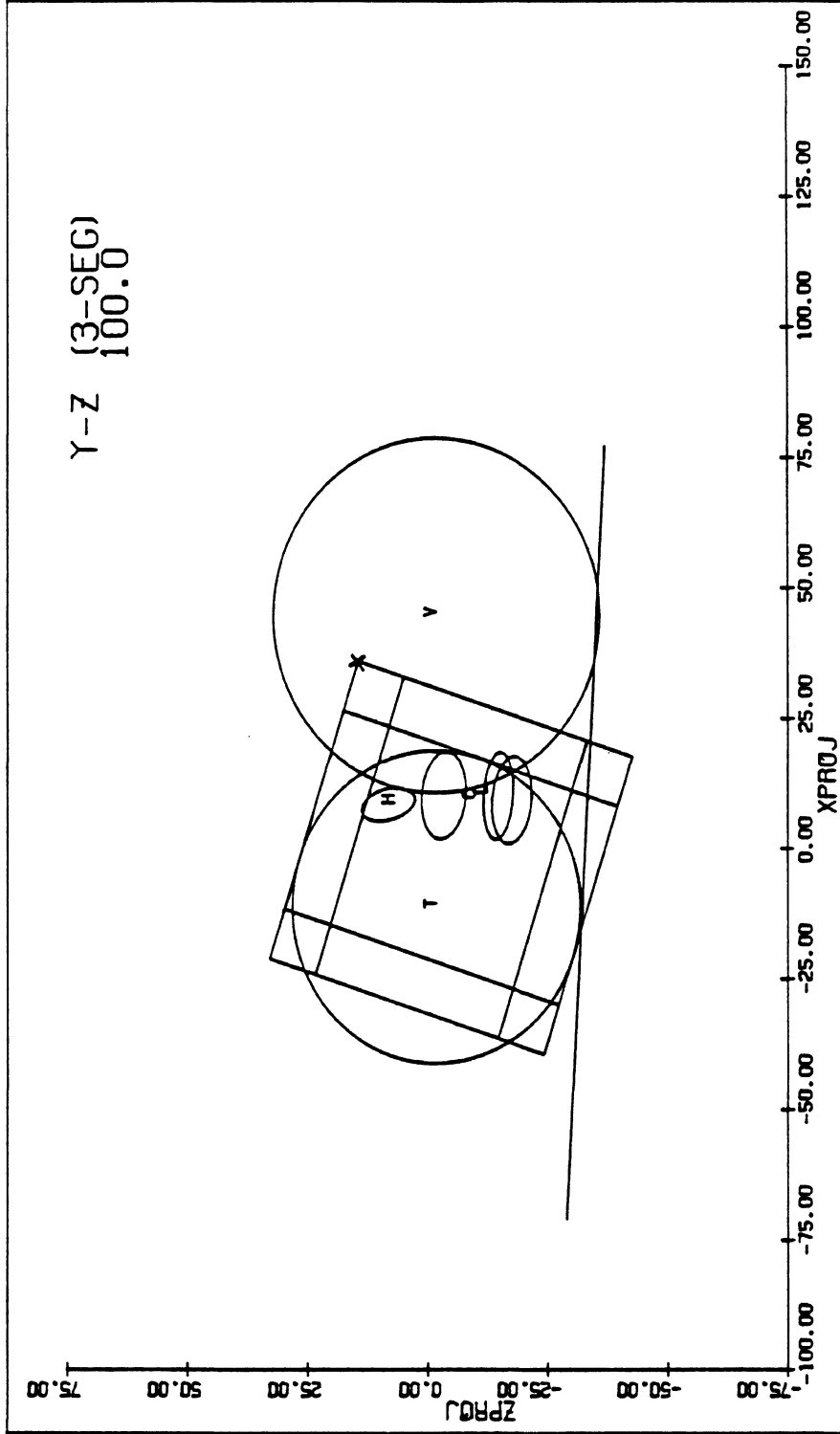


FIGURE 3. Simple rollover simulation. Time = 100 milliseconds.

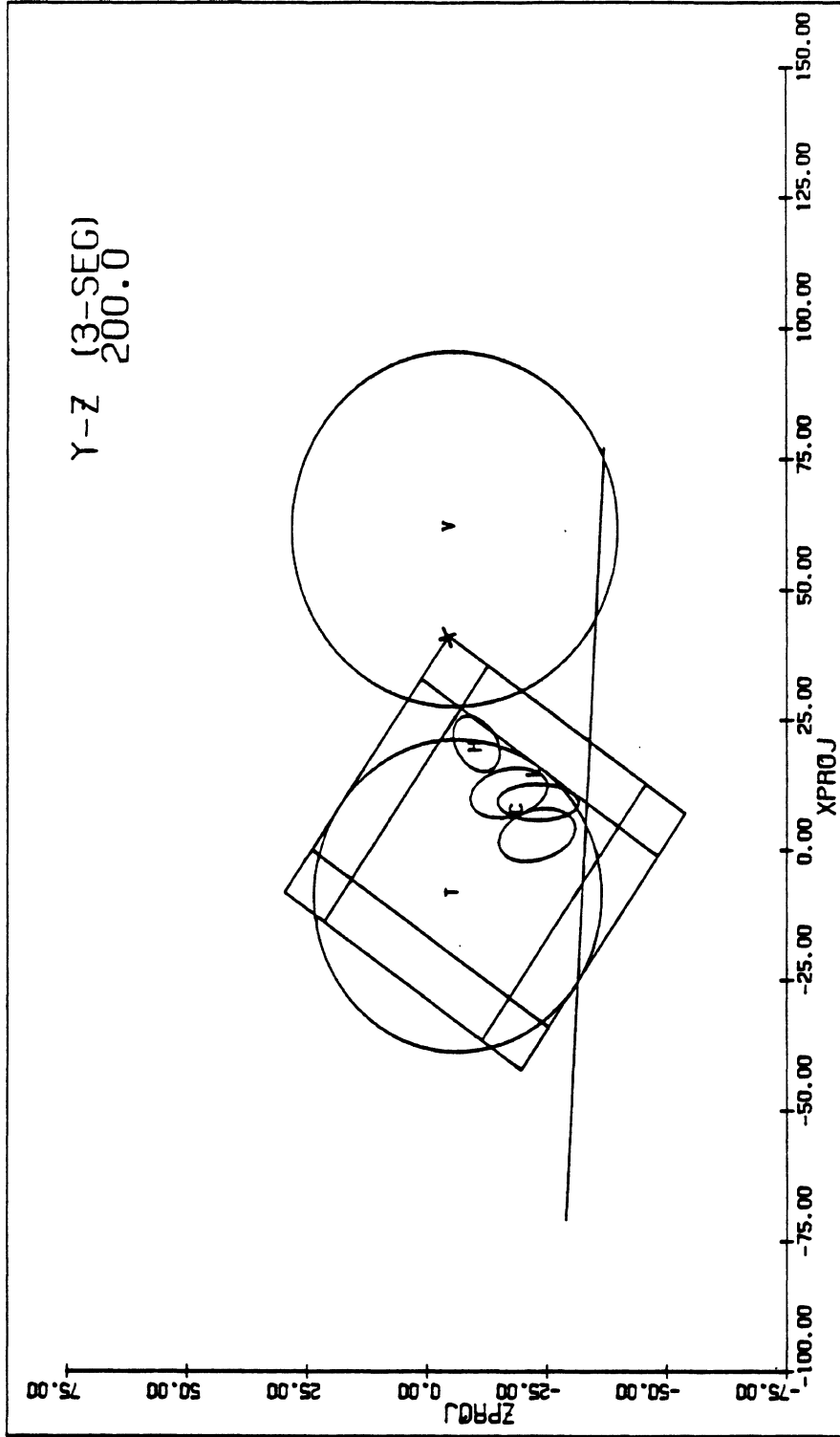


FIGURE 4. Simple rollover simulation. Time = 200 milliseconds.

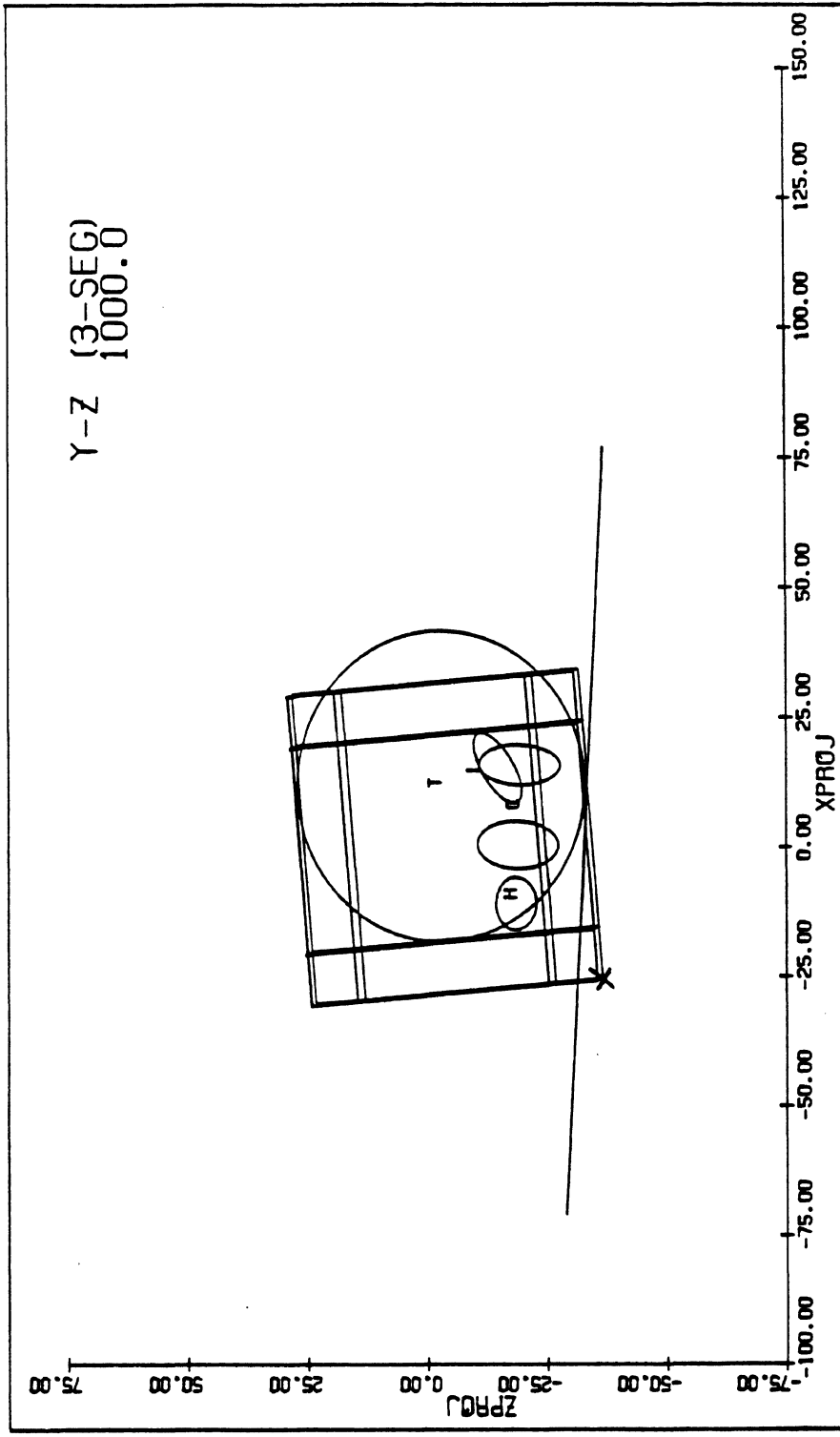


FIGURE 5. Simple rollover simulation. Time = 1000 milliseconds.



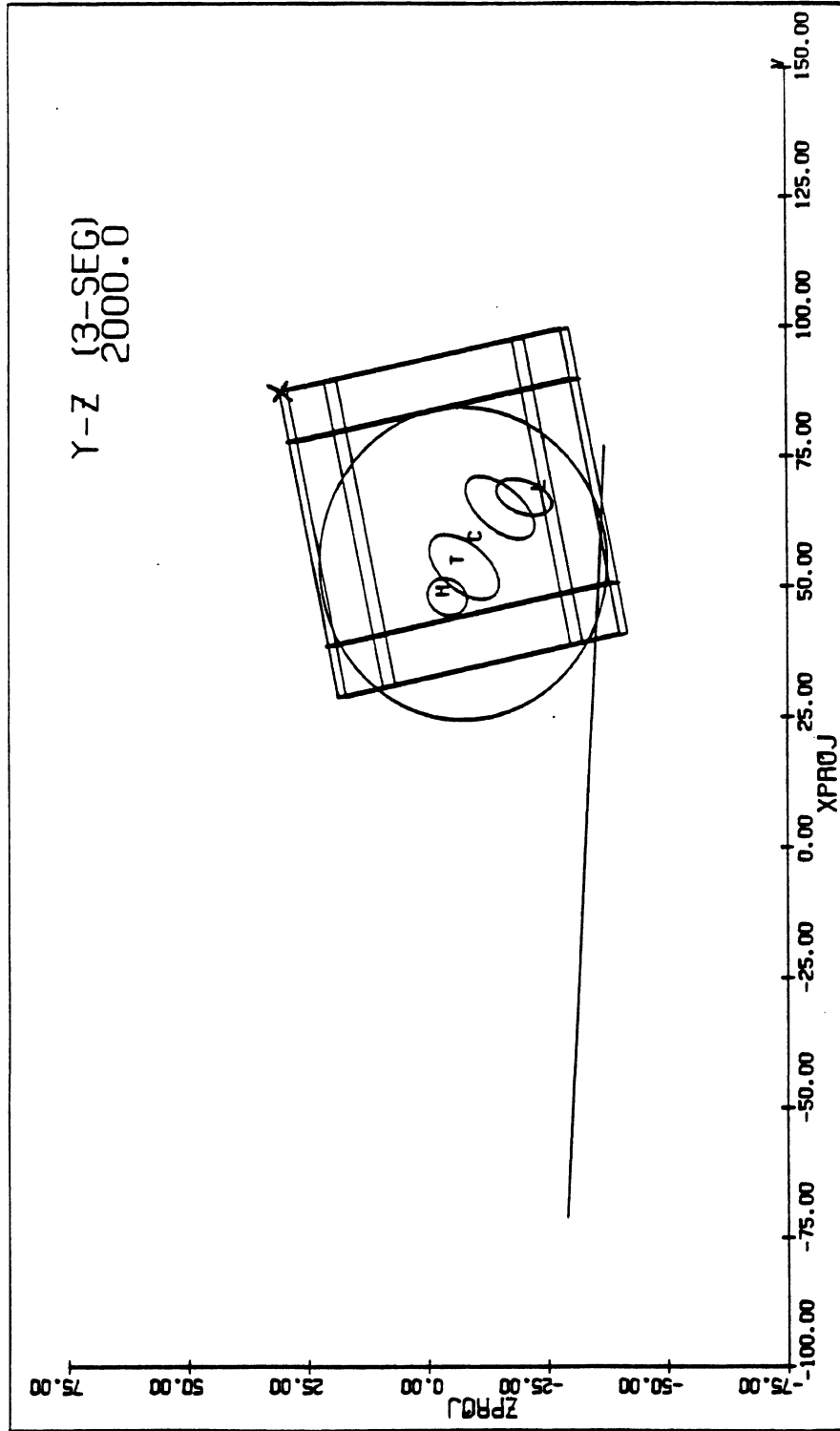


FIGURE 6. Simple rollover simulation. Time = 2000 milliseconds.

TABLE 1

## HEAD/VEHICLE INTERACTION FORCES (SIMPLE ROLLOVER)

Vehicle Component	Time Duration (ms)	Peak Force (N)
Roof	0-170	4615
Driver Door	170-190	3653
Driver Door	250-360	1940
Instrument Panel	310-370	2768
Roof	840-950	2461
Driver Door	930-950	979
Driver Door	1210-1240	1259
Seat Back	1460-1550	2817
Passenger Door	1500-1540	3827
Instrument Panel	1770-1890	5732
Passenger Door	1790-2000	3800
Floor	1810-1850	6519

TABLE 2

## CHEST/VEHICLE INTERACTION FORCES (SIMPLE ROLLOVER)

Vehicle Component	Time Duration (ms)	Peak Force (N)
Floor	310-370	6226
Driver Door	330-350	823
Roof	940-990	3289
Seat Back	1580-1620	1446

TABLE 3

## HIP/VEHICLE INTERACTION FORCES (SIMPLE ROLLOVER)

Vehicle Component	Time Duration (ms)	Peak Force (N)
Driver Door	70-130	5006
Floor	300-350	2657
Floor	390-450	1331
Seat Back	470-530	2136
Floor	650-700	2092
Roof	980-1020	4739
Roof	1380-1430	3573
Passenger Door	1400-1440	4877
Driver Door	1610-1670	8001
Seat Back	1640-1690	7022

TABLE 4

## THIGH/VEHICLE INTERACTION FORCES (SIMPLE ROLLOVER)

Vehicle Component	Time Duration (ms)	Peak Force (N)
Driver Door	130-190	2857
Seat Back	220-280	1558
Driver Door	290-380	5607
Floor	430-500	1780
Floor	660-710	1566
Passenger Door	1100-1170	2212
Roof	1350-1410	5304
Instrument Panel	1370-1430	5340
Driver Door	1650-1670	579
Floor	1680-2000	2648

**TABLE 5**  
**PEAK ACCELERATION EXCEEDING 10 G's FOR HEAD (SIMPLE ROLLOVER)**

Time (ms)	Peak G	Interaction*
130	30	Roof
180	41	Driver Door
250	19	Driver Door
340	30	Driver Door, Instrument Panel
850	20	Roof
900	11	Roof
1220	11	Driver Door
1410	12	(Hip vs. Roof and Passenger Door)
1460	47	Seat Back
1480	53	Seat Back
1510	49	Passenger Door, Seat Back
1630	12	(Hip vs. Driver Door and Seat Back)
1680	11	(Hip vs. Driver Door and Seat Back)
1810	108	Floor, Passenger Door, Instrument Panel

**TABLE 6**  
**PEAK ACCELERATION EXCEEDING 10 G's FOR TORSO (SIMPLE ROLLOVER)**

Time (ms)	Peak G	Interaction*
100	11	Hip vs. Driver Door
330	17	Hip vs. Floor; Chest vs. Driver Door and Floor
1410	13	Hip vs. Passenger Door and Floor
1650	17	Hip vs. Driver Door and Seat Back
1830	12	(Head vs. Floor, Passenger Door, and Instrument Panel)

\*Items shown in parenthesis indicate a large force on an adjacent body segment which at the same time is transferring forces through the linkage.

**TABLE 7**  
**PEAK ACCELERATION EXCEEDING 10 G's FOR LEGS (SIMPLE ROLLOVER)**

Time (ms)	Peak G	Interaction
150	11	Thigh vs. Inner Door
340	17	Thigh vs. Inner Door
1390	23	Thigh vs. Roof
1660	11	Thigh vs. Inner Door, Floor, and Instrument Panel

## 4.0 FULL-SCALE ROLLOVER SIMULATION

The purpose of this section of the report is to describe the three-dimensional simulation of a rollover event that has been the subject of a previous simulation effort using the MVMA 2-D model (4,5). The three-dimensional baseline data set has been developed and exercised. In addition to presentation and evaluation of simulation results, recommendations are given for their improvement.

### 4.1 VEHICLE DESCRIPTION

Figure 7 is a schematic view of the initial configuration of a driver in a vehicle ready for a dolly drop rollover test. This configuration was used for the MVMA 2-D simulation discussed earlier in the report. Figure 8 identifies the surfaces selected to interact with the occupant during the crash event. These same data were used in the preparation of the three-dimensional data set. Figures 9, 10, and 11 show the three plane views of occupant and contact surfaces that were selected for the initial rollover simulation in three dimensions.

The driver door (D DOOR) and passenger door (P DOOR) shown in Figure 9 are idealized from the two-dimensional case to represent the first step in a fully three-dimensional simulation of an unrestrained driver. The location of the plane of the steering wheel is also included. All surfaces are idealized representations of the configuration of an anthropomorphic test device in the driver position of a 1973 Buick prior to the dolly drop test conducted at the General Motors Proving Grounds.

### 4.2 OCCUPANT DESCRIPTION

A basic input data set, provided by General Motors, was used in this study to describe a Hybrid III dummy. This same data set has been used in studies of three-dimensional belt (2) and steering assembly (1) modeling. The dummy data and the remainder of the information required for this simulation are included in the Table 8 listing.

Figure 12 illustrates the ellipsoids that have been attached to each body segment for possible use in sensing contacts with the various vehicle interior components. Table 9 lists these body segments in the order they are included in the data set describing the open linkage of rigid bodies.

Table 10 is a list of the occupant contacts that are allowed with the various vehicle interior components. These are listed in the order of the contact surfaces defined on the D.2 cards in the input data set. Each of these contacts is defined by one of the F.1 cards in the data set.

X-Z INERTIAL  
0.0

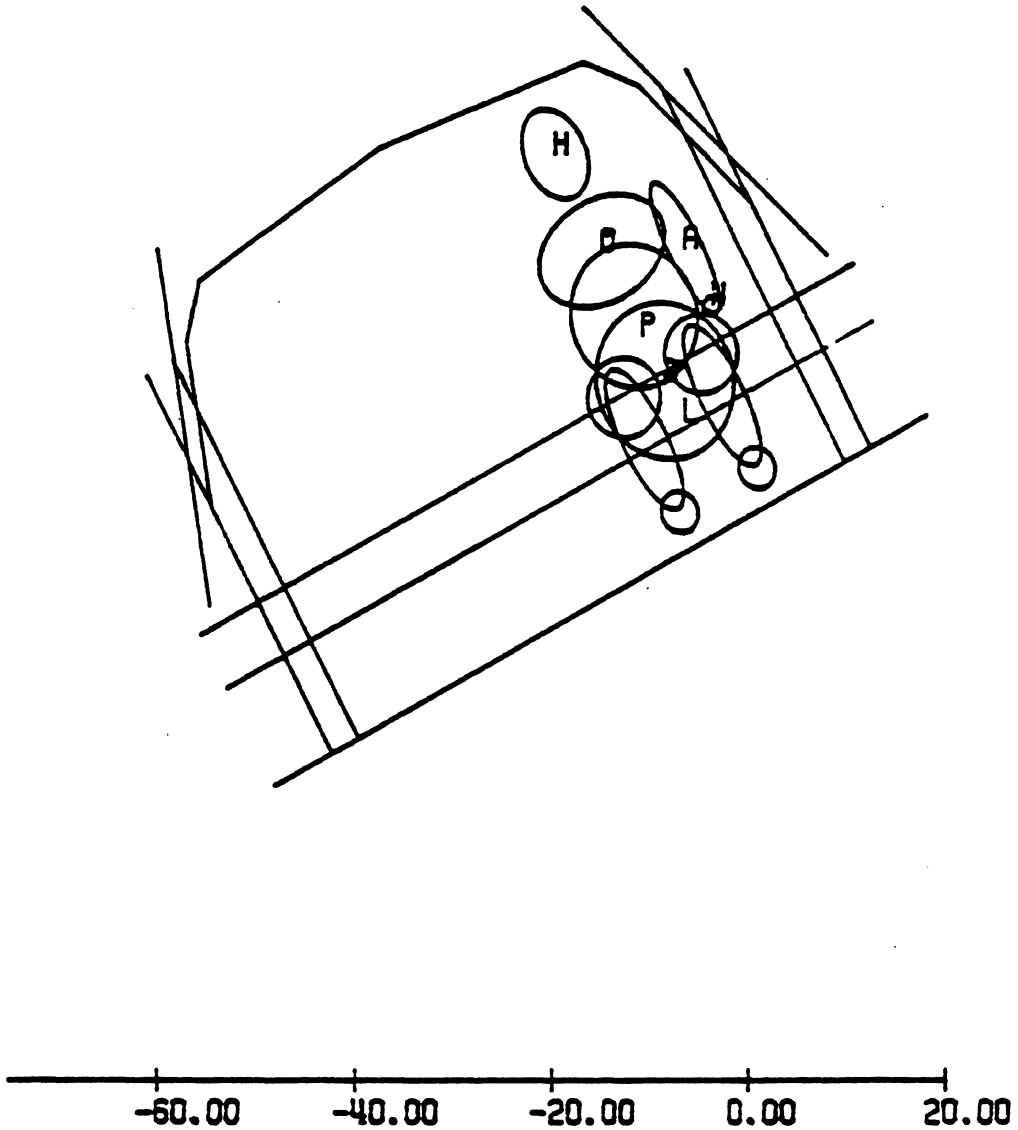
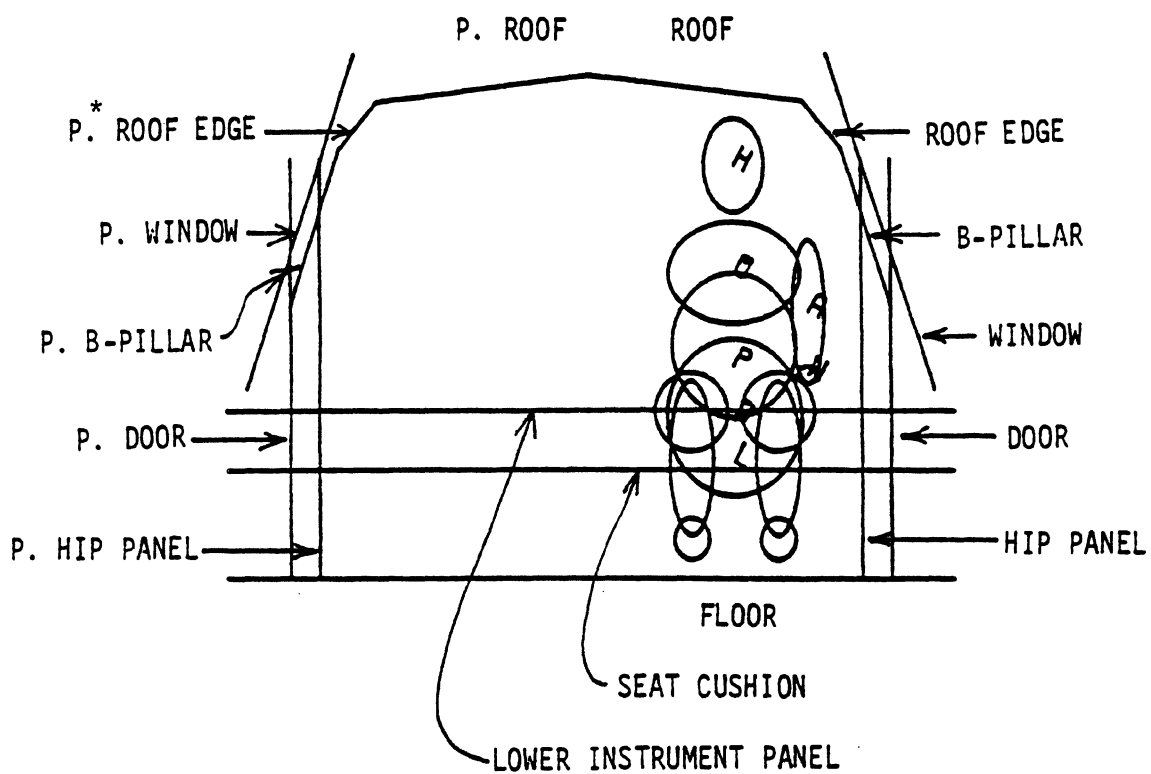


FIGURE 7. Initial MVMA 2-D configuration of occupant in vehicle for simulation of dolly drop rollover.



\*THE LETTER "P" REFERS TO PASSENGER SIDE OF VEHICLE.

FIGURE 8. MVMA 2-D vehicle interior contact surfaces (view from front).

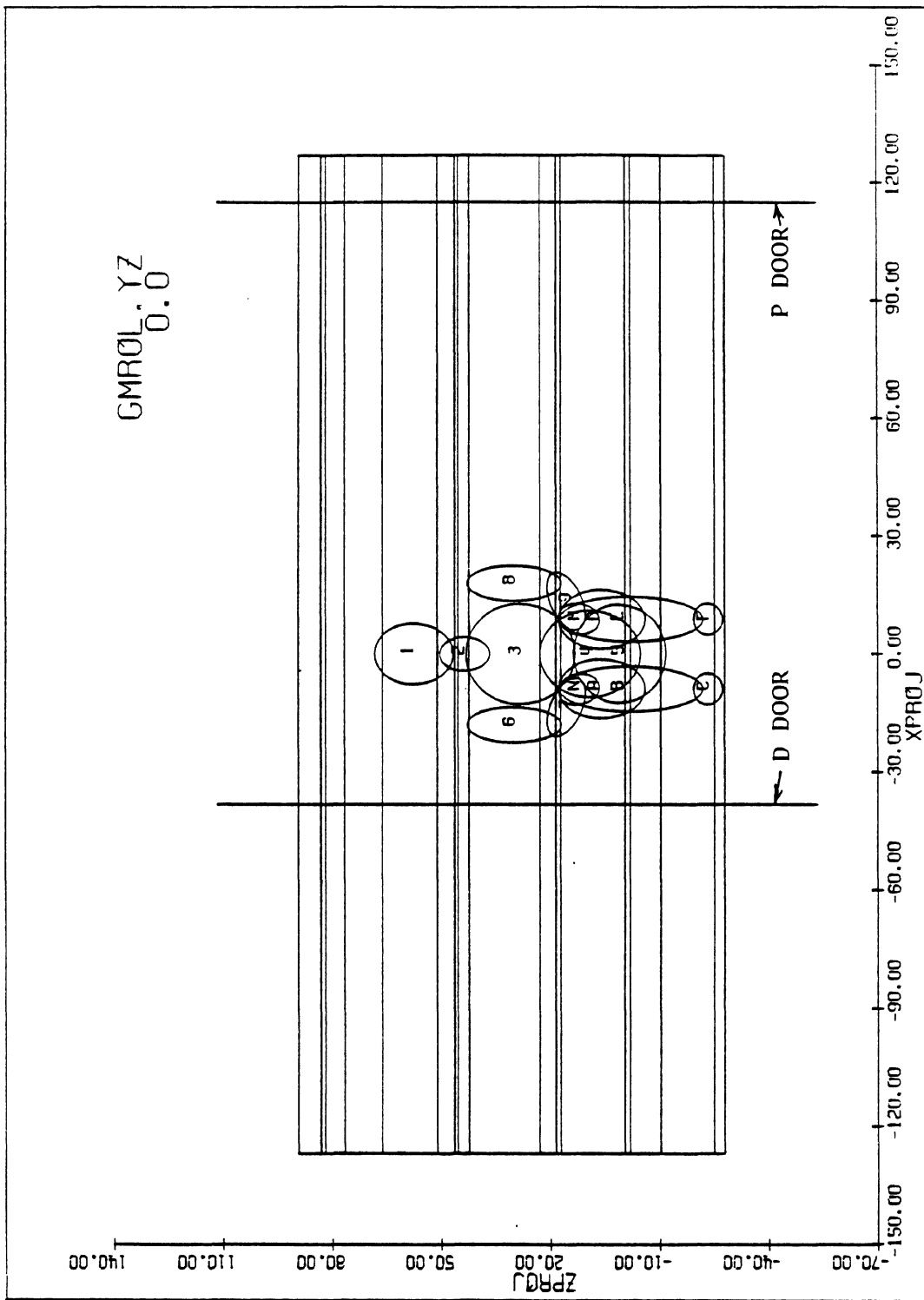


FIGURE 9. Rear view of 3-D occupant in vehicle (Y-Z plane).



GMR0L XZ  
0.0

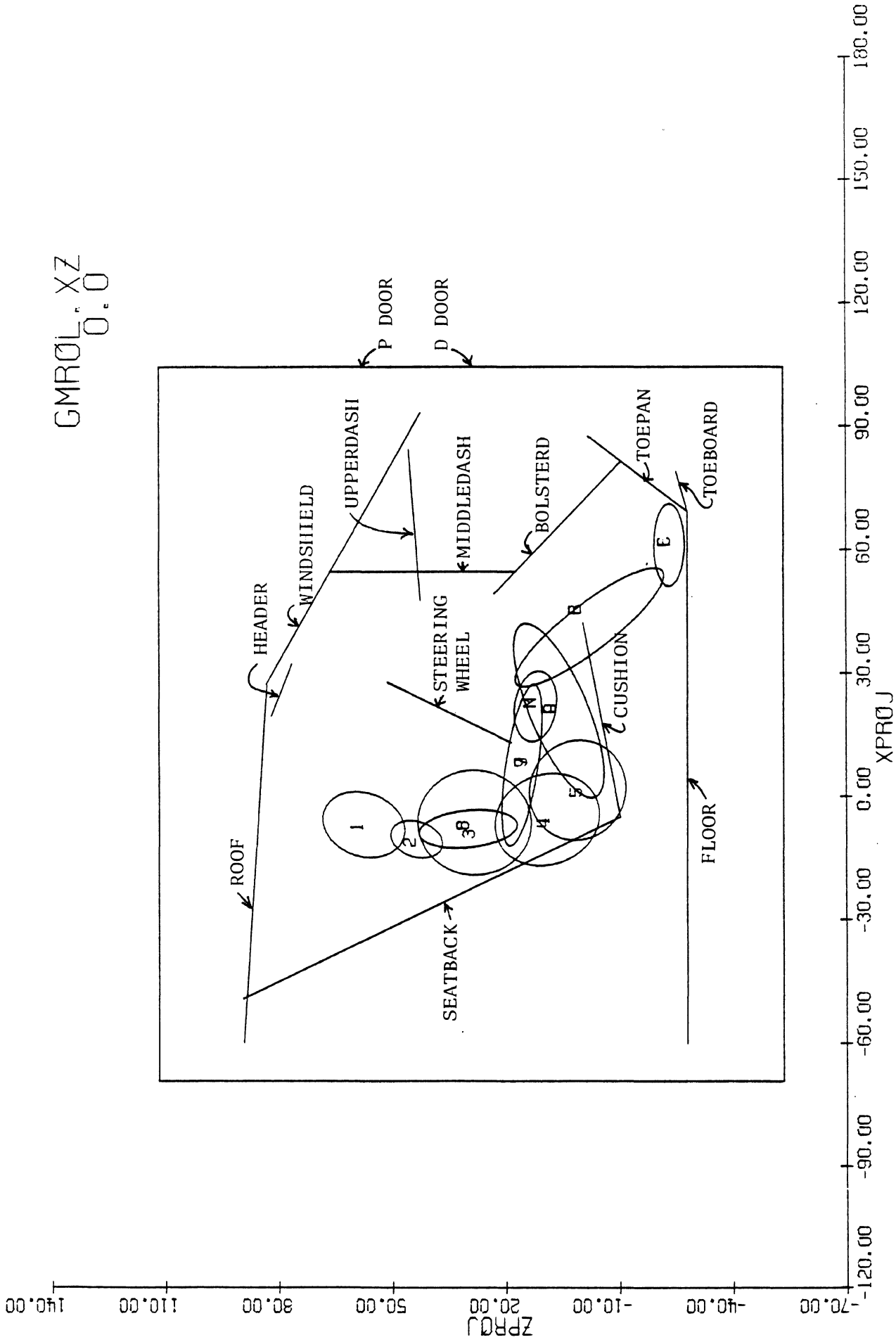


FIGURE 10. Side view of 3-D occupant in vehicle (X-Z plane).

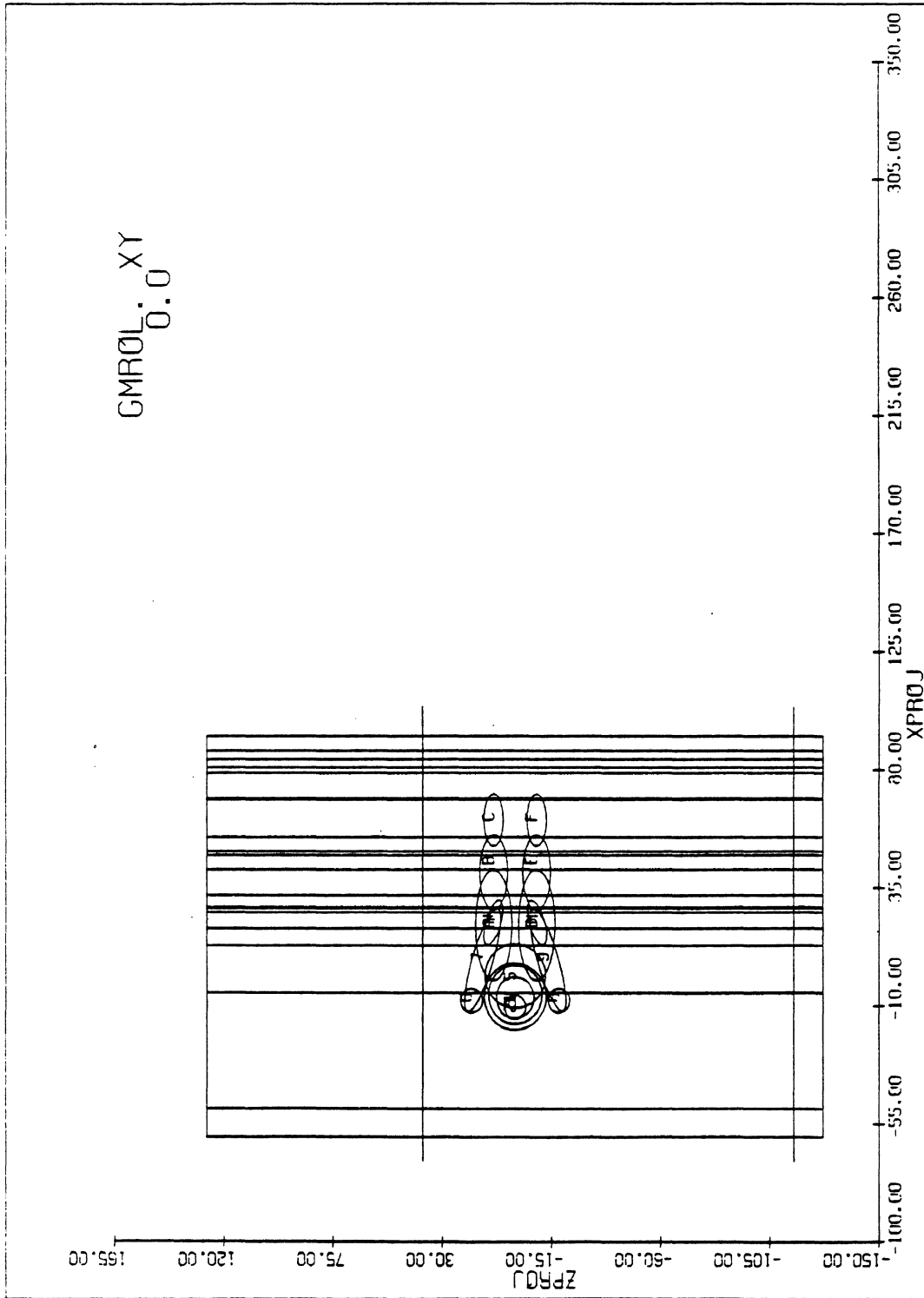


FIGURE 11. Top view of 3-D occupant in vehicle (X-Y plane).

GMR0L XZ  
0.0

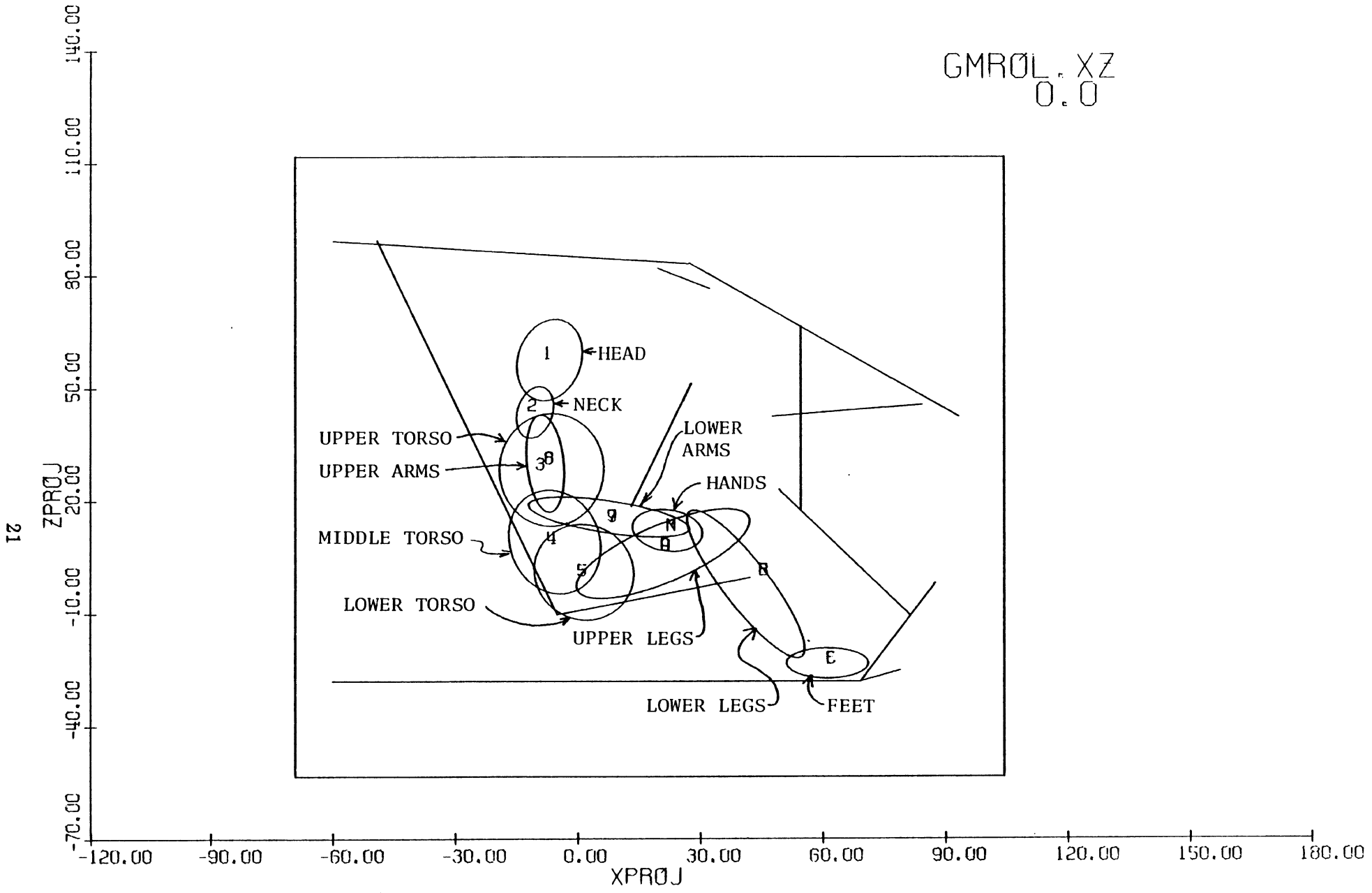


FIGURE 12. Occupant contact ellipsoids.







175		69.19	127.00	27.97					3 D.2.B
177		87.48	127.00	1.88					3 D.2.C
177.5		69.19	-127.00	27.97					3 D.2.D
178	4	BOLSTERD							4 D.2.A
179		48.97	127.00	-23.04					4 D.2.B
181		48.97	-127.00	-23.04					4 D.2.D
181.5		81.08	127.00	10.34					4 D.2.C
182	5	MIDDLEDASH							5 D.2.A
183		54.43	127.00	-66.35					5 D.2.B
185		54.43	-127.00	-66.35					5 D.2.D
185.5		54.43	127.00	-17.22					5 D.2.C
186	6	UPPERDASH							6 D.2.A
187		84.15	127.00	-45.62					6 D.2.B
189		84.15	-127.00	-45.62					6 D.2.D
189.5		47.50	127.00	-42.42					6 D.2.C
190	7	WINDSHIELD							7 D.2.A
191		27.18	127.00	-83.24					7 D.2.B
193		27.18	-127.00	-83.24					7 D.2.D
193.5		93.04	127.00	-42.42					7 D.2.C
194	8	CUSHION							8 D.2.A
195		42.16	127.00	0.36					8 D.2.B
197		42.16	-127.00	0.36					8 D.2.D
197.5		-4.91	127.00	10.24					8 D.2.C
198	9	SEATBACK							9 D.2.A
199		-4.91	127.00	10.24					9 D.2.B
201		-4.91	-127.00	10.24					9 D.2.D
201.5		-49.15	127.00	-89.29					9 D.2.C
202	10	HEADER							10 D.2.A
203		19.56	127.00	-81.94					10 D.2.B
205		19.56	-127.00	-81.94					10 D.2.D
205.5		32.26	127.00	-76.63					10 D.2.C
206	11	ROOF							11 D.2.A
207		-60.00	127.00	-89.29					11 D.2.B
209		-60.00	-127.00	-89.29					11 D.2.D
209.5		27.18	127.00	-83.24					11 D.2.C
210	12	STEERINGWHEEL							12 D.2.A
211		27.81	127.00	-51.23					12 D.2.B
213		27.81	-127.00	-51.23					12 D.2.D
213.5		13.03	127.00	-18.62					12 D.2.C
214	13	RIMTOP							13 D.2.A
215		27.81	127.00	-51.23					13 D.2.B
217		25.70	127.00	-46.52					13 D.2.C
217.5		27.81	-127.00	-51.23					13 D.2.D
218	14	D DOOR							14 D.2.A
219		104.39	-38.0	-111.63					14 D.2.B
220		-69.34	-38.0	-111.63					14 D.2.C
221		104.39	-38.0	53.37					14 D.2.D
222	15	P DOOR							15 D.2.A
223		104.39	115.0	-111.63					15 D.2.B
224		104.39	115.0	53.37					15 D.2.D
225		-69.34	115.0	-111.63					15 D.2.C
225.5									D.7
226	1	DASHSTAT							1 E.1
227	O	1000000.	O						1 E.2
228		78.796639	-7.7087884	O.2596744	O.0018579				1 E.3
229	2	CUSHIONSTAT							2 E.1
230	O	1000000.	O						2 E.2
231		26.25126	2.643656	-2.0616064	O.241544				2 E.3

TABLE 8 (Continued)





291	5	18	3	3	1	-1	14	13	12	5	F.1.B	
292	5	18	5	5	1	-1	14	13	12	5	F.1.C	
293	5	18	6	6	1	-1	14	13	12	5	F.1.D	
294	5	18	9	9	1	-1	14	13	12	5	F.1.E	
295.1	7	18	1	1	1	-1	14	13	12			
296	7	18	3	3	5	-1	14	13	12	7	F.1.B	
297	7	18	5	5	5	-1	14	13	12	7	F.1.C	
297.1	7	18	6	6	5	-1	14	13	12			
297.2	7	18	9	9	5	-1	14	13	12			
298	8	18	1	1	2	-1	14	13	12	8	F.1.B	
298.1	8	18	3	3	2	-1	14	13	12			
298.2	8	18	5	5	2	-1	14	13	12			
299	8	18	6	6	2	-1	14	13	12	8	F.1.C	
300	8	18	9	9	2	-1	14	13	12	8	F.1.D	
301	9	18	1	1	3	-1	14	13	12	9	F.1.B	
302	9	18	3	3	3	-1	14	13	12	9	F.1.C	
302.1	9	18	5	5	3	-1	14	13	12			
302.2	9	18	6	6	3	-1	14	13	12			
302.3	9	18	9	9	3	-1	14	13	12			
305.1	11	18	1	1	9	-1	14	13	12			
305.2	11	18	3	3	9	-1	14	13	12			
306	11	18	5	5	9	-1	14	13	12	11	F.1.C	
306.1	11	18	6	6	9	-1	14	13	12			
306.2	11	18	9	9	9	-1	14	13	12			
307	14	18	1	1	10	-1	14	13	12	14	F.1.B	
308	14	18	3	3	10	-1	14	13	12	14	F.1.C	
309	14	18	5	5	10	-1	14	13	12	14	F.1.D	
310	14	18	6	6	10	-1	14	13	12	14	F.1.E	
311	14	18	7	7	10	-1	14	13	12	14	F.1.F	
312	15	18	1	1	11	-1	14	13	12	15	F.1.B	
313	15	18	3	3	11	-1	14	13	12	15	F.1.C	
314	15	18	5	5	11	-1	14	13	12	15	F.1.D	
315	15	18	9	9	11	-1	14	13	12	15	F.1.E	
316	15	18	10	10	11	-1	14	13	12	15	F.1.F	
317											F.3	
317.5											F.4	
318	10.0		30.0		1.0						G.1.A	
319		0.0	0.0		-115.8						G.2.A	
320	0.0		22.50		0.0					18	G.3.A	
321	0.0		15.00		0.0					18		
322	0.0		-2.00		0.0					18		
323	0.0		-15.00		0.0					18		
324	0.0		-15.0		0.0					18		
325	0.0		115.00		0.0					18		
326	0.0		35.000		0.0					18		
327	0.0		90.0		0.0					18		
328	0.0		115.00		0.0					18		
329	0.0		35.000		0.0					18		
330	0.0		90.0		0.0					18		
331	0.0		5.0		0.					18		
332	17.5		81.0		0.	0.0	0.0	0.0	3	2	1	18
333	0.0		5.0		00.							18
334	-17.5		81.0		0.				3	2	1	18
335	17.5		81.0		0.				3	2	1	18
336	-17.5		81.0		0.				3	2	1	18
1001	0.		2000.		0.							H.O.1
1002	1	2	3	4	5	6	7	8				H.O.2
1003												H.O.3

TABLE 8 (Continued)



H.7

	12	13	14	15	16
1063	0	1	1	0	3
2001	0	2	0	0	.05
2002	0	0	0	0	0
2003	1	0	0	0	0
2004	0	1	0	0	0
2005	0	0	1	0	0
2006	1	0	0	1	0
2007	0	1	0	0	0
2008	0	1	0	0	0
2009	0	0	1	0	0
2010	.5	.5	11.	8.5	
2011	.5	.5	10.	7.	
2012	-100.	-115.	250.	175.	.3
2013	GMRDL.	XZ			
2014	0	-1.	0	0	
2015	1	0	0	0	
2016	0	0	1	0	
2017	.5	9.	11.	8.5	
2018	.5	.5	10.	7.	
2019	-150.	-140.	300.	210.	.3
2020	GMRDL.	VZ			
2021	1.	0	0	0	
2022	0	0	1	0	
2023	0	-1.	0	0	
2024	.5	17.5	11.	8.5	
2025	.5	.5	10.	7.	
2026	-100.	-150.	450.	315.	.3
2027	GMRDL.	XY			

TABLE 8 (Continued)

TABLE 9

## LIST OF DUMMY SEGMENTS AND CONTACT ELLIPSOIDS

Segment Number	Segment Name (Segment Code)
1	Lower torso (LT)
2	Middle torso (MT)
3	Upper torso (UT)
4	Neck (N)
5	Head (H)
6	Left upper leg (LUL)
7	Left lower leg (LLL)
8	Left foot (LF)
9	Right upper leg (RUL)
10	Right lower leg (RLL)
11	Right foot (RF)
12	Left upper arm (LUA)
13	Left lower arm (LLA)
14	Right upper arm (RUA)
15	Right lower arm (RLA)
16	Left hand (LH)
17	Right hand (RH)

TABLE 10

## LIST OF ALLOWED OCCUPANT CONTACTS WITH THE VEHICLE

Vehicle Segment (number)	Occupant Segment
FLOOR (1)	Left Lower leg Right lower leg
TOEBOARD (2)	
TOEPAN (3)	Left lower leg Right lower leg
BOLSTERD (4)	Left upper leg Left lower leg Right upper leg Right lower leg
MIDDLEDASH (5)	Lower torso Upper torso Head Left upper leg Right upper leg
UPPERDASH (6)	
WINDSHIELD (7)	Lower torso Upper torso Head Left upper leg Right upper leg
CUSHION (8)	Lower torso Upper torso Head Left upper leg Right upper leg
SEATBACK (9)	Lower torso Upper torso Head Left upper leg Right upper leg
HEADER (10)	
ROOF (11)	Upper torso Lower torso Head Left upper leg Right upper leg

TABLE 10 (Continued)

Vehicle Segment (number)	Occupant Segment
STEERINGWHEEL (12)	
RIMTOP (13)	
D DOOR (14)	Lower torso Upper torso Head Left upper leg Left lower leg
P DOOR (15)	Lower torso Upper torso Head Right upper leg Right lower leg

It should be noted that there are 17 ellipsoids modeling the surface of the dummy and 15 surfaces modeling the interior of the vehicle. If all ellipsoids were allowed to contact all interior surfaces, a total of 255 force interactions would be computed at each time step whether the force was zero or not. Experience with crash victim simulation models has shown that computational time is highly correlated with the number of contact interactions that are included. Because of this, the number was reduced to the 43 interactions that were believed to be the most basic for this initial full-scale simulation. A primary criterion in selecting those contacts which are to be allowed and those which are not is to choose those that appear to be the most critical to overall containment of the occupant inside the vehicle. The five believed to meet this criterion, and which are very often involved in serious injury, are the head, upper torso, lower torso, left upper leg, and right upper leg. After completion of this first simulation, and to proceed toward the goal of an improved representation of the dynamic event, surfaces that are observed to be needed can be added, while those seen to be inactive in force production can be deleted. This process helps to reduce CPU time, the quantity of output, and time required for analysis of results.

### 4.3 VEHICLE MOTION

The data for the description of vehicle motion were available from an analysis of high-speed films. The dolly drop rollover test was idealized to be a pure roll. The three active degrees of freedom of vehicle motion included horizontal, vertical, and roll components. It was necessary to use the spline-fit option included with the GMCVS for describing this complex crash situation. Plots of the data are included as Figures 13, 14, and 15. The data used for the MVMA 2-D simulation are superimposed on these plots. It should be noted that more points are included for use with GMCVS than for MVMA 2-D. This is because the input for GMCVS requires data for all six degrees of freedom of motion at any time point for which motion is prescribed.

### 4.4 RESULTS

This section summarizes the results generated during the full-scale rollover simulation. The results include tabulations of contact forces between the occupant and the vehicle, G-loadings on the various segments of the simulated occupant, and graphical displays of occupant motions. Motions observed during the rollover test are compared qualitatively with the simulated results.

Table 11 lists the contact forces between the occupant and the vehicle. All contacts that are specified in the input data set are included whether or not a non-zero force was generated. Table 12 lists the peak G-loadings greater than 10 acting on each segment. The key to the code used for body segments has been given in Table 9.

In this partial simulation of a complete rollover, most of the non-zero contacts are with the seat, roof, windshield, and floor. An examination of Tables 11 and 12 shows that the largest G-loadings are the result of direct contact between an occupant segment and a vehicle surface. A secondary effect is observed when the effect of a particular loading is transmitted to neighboring links in the body chain. This is particularly noticeable for the contact of the two upper leg segments with the windshield. The peak load of 1181 kilograms force is reached at 459 milliseconds for the left upper leg while the peak is

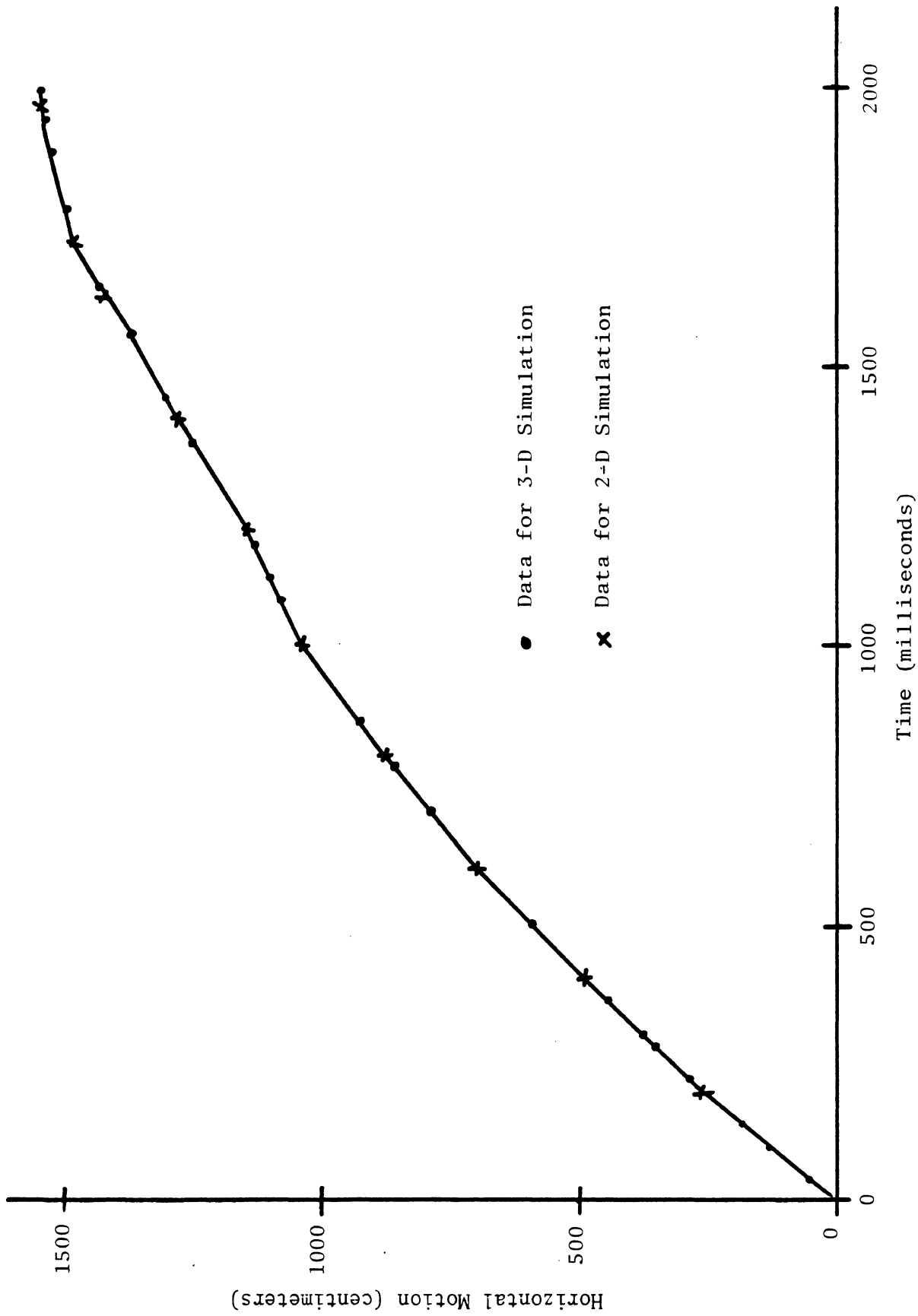


FIGURE 13. Horizontal motion of vehicle.



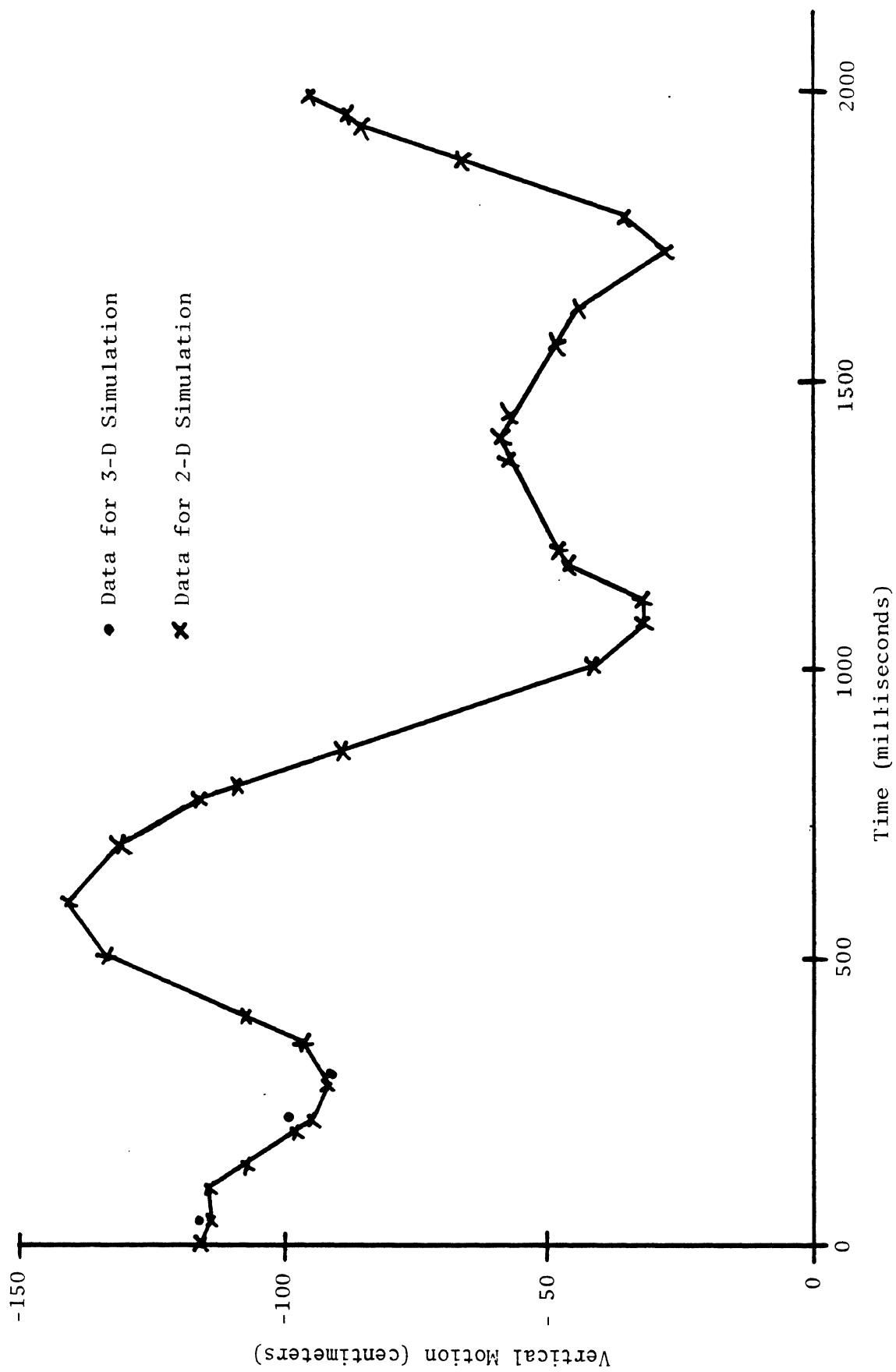


FIGURE 14. Vertical motion of vehicle.

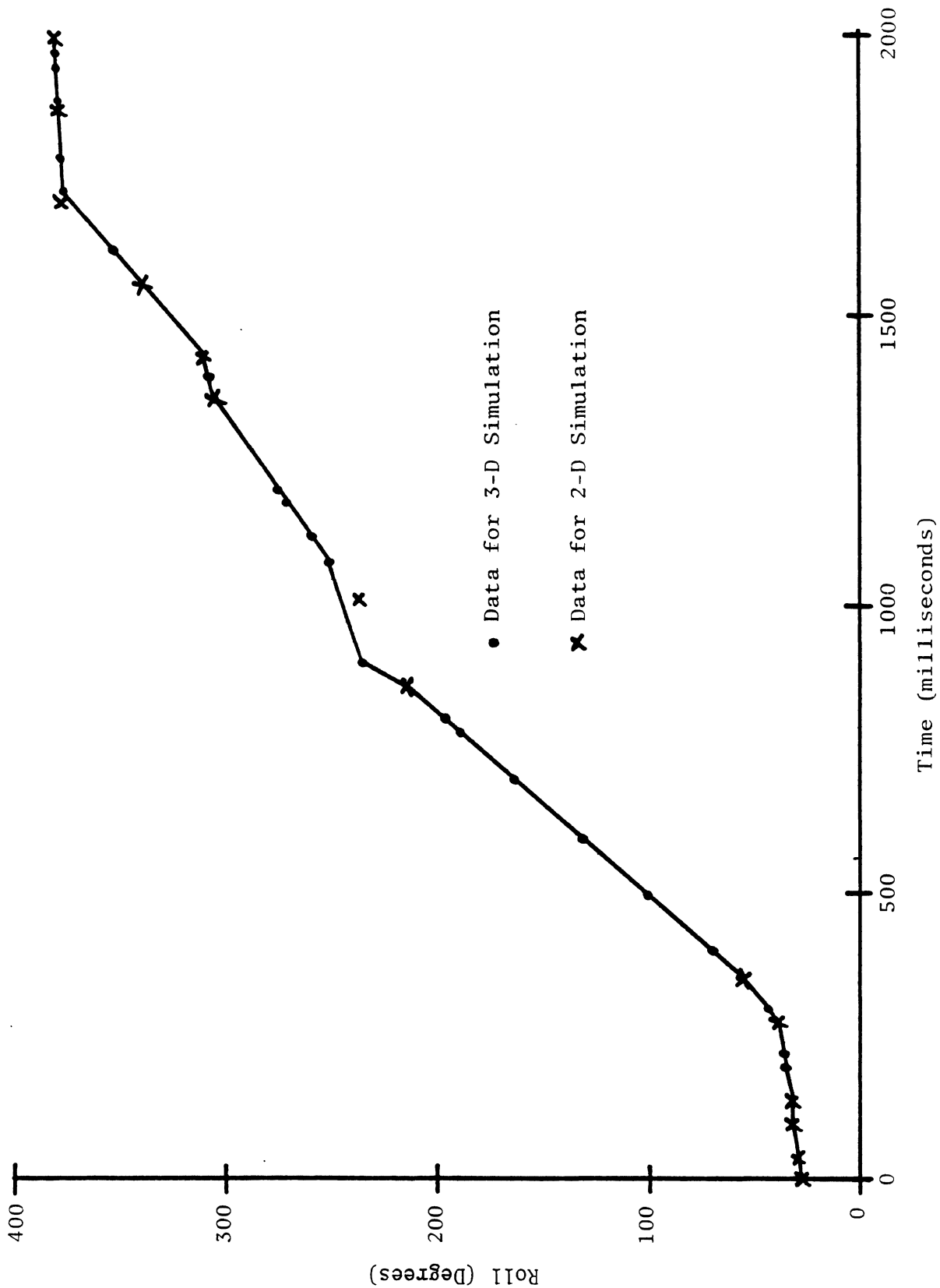


FIGURE 15. Roll angle of vehicle.

TABLE 11

## CONTACT FORCES BETWEEN OCCUPANT AND VEHICLE

Vehicle Surface	Body Segment	Start Time (ms)	Max Value (kgf)	Time at Max (ms)	End Time (ms)
FLOOR	LLL	41	198	51	53
	RLL	44	161	53	55
TOEPAN	LLL	—	—	—	—
	RLL	—	—	—	—
BOLSTERD	LUL	—	—	—	—
	LLL	—	—	—	—
	RUL	—	—	—	—
	RLL	—	—	—	—
MIDDLEDASH	LT	—	—	—	—
	UT	—	—	—	—
	H	—	—	—	—
	LUL	—	—	—	—
	RUL	—	—	—	—
WINDSHIELD	LT	—	—	—	—
	UT	—	—	—	—
	H	—	—	—	—
	LUL	450	1181	459	462
	RUL	453	1505	463	465
	RUL	504	204	504	504
CUSHION	LT	0	484	57	69
	UT	—	—	—	—
	H	—	—	—	—
	LUL	21	53	54	62
	RUL	21	87	57	66
SEATBACK	LT	0	36	68	83
	UT	29	24	84	95
	H	480	28	504	504
	LUL	—	—	—	—
	RUL	—	—	—	—
ROOF	UT	464	898	486	491
	LT	—	—	—	—
	H	384	430	402	405
	H	409	443	429	504
	LUL	—	—	—	—
	RUL	—	—	—	—

Vehicle Surface	Body Segment	Start Time (ms)	Max Value (kgf)	Time at Max (ms)	End Time (ms)
D DOOR	LT	—	—	—	—
	UT	—	—	—	—
	H	—	—	—	—
	LUL	—	—	—	—
	LLL	—	—	—	—
P DOOR	LT	—	—	—	—
	UT	—	—	—	—
	H	—	—	—	—
	RUL	—	—	—	—
	RLL	—	—	—	—

TABLE 12  
PEAK RESULTANT G-LOADINGS ON OCCUPANT

Segment	Peak (G's)	Time (ms)	Segment	Peak (G's)	Time (ms)
Lower Torso	11	54	Right Upper Leg	22	53
	74	460		156	461
	16	476		20	504
	17	483	Right Lower Leg	43	54
	28	504		154	461
Center Torso	10	56	17	477	
	11	355	27	504	
	42	460	Right Foot	51	54
	25	475		121	457
	66	504	Left Upper Arm	12	56
Upper Torso	10	412		29	356
	10	421		41	365
	10	428		51	370
	11	456		60	486
	13	461	374	504	
33	487	Left Lower Arm	22	339	
20	504		113	355	
Neck	16		355	115	364
	23		364	80	370
	13		369	20	389
	11	403	24	474	
	12	412	54	481	
13	421	749	504		
13	428	Right Upper Arm	11	57	
12	437		17	355	
15	456		14	370	
50	486		10	457	
117	504		63	480	
Head	73	397	91	504	
	13	441	Right Lower Arm	12	355
	21	445		21	474
	27	453		50	480
	22	466		46	504
	30	472		Left Hand	48
	35	481	455		364
	12	496	85		389
	45	504	27		474
	Left Upper Leg	24	52		58
135		459	1471	504	
11		504			

TABLE 12 (Continued)

Segment	Peak (G's)	Time (ms)	Segment	Peak (G's)	Time (ms)
Left Lower Leg	36	50	Right Hand	11	355
	131	454		18	474
	11	504		48	480
		49		504	
Left Foot	38	50			
	119	454			

1505 kilograms force at 463 milliseconds for the right upper leg. Forces from this overall loading are transmitted into the linkage as follows:

- Left upper leg (135 G's at 459 milliseconds)
- Right upper leg (156 G's at 463 milliseconds)
- Lower torso (74 G's at 460 milliseconds)
- Middle torso (42 G's at 460 milliseconds)
- Upper torso (13 G at 461 milliseconds)
- Left lower leg (131 G's at 454 milliseconds)
- Left foot (119 G's at 454 milliseconds)
- Right lower leg (154 G's at 461 milliseconds)
- Right foot (121 G's at 457 milliseconds)

A reduction in the G-loading is observed for segments progressively further from the upper leg segments. The fact that the peak loads transmitted to the lower legs and feet appear to occur earlier than the values for the upper legs is due to:

- their smaller mass,
- the fact that the load is applied over a period of time starting about 10 milliseconds before peak acceleration, and
- inertial effects.

A different phenomenon is observed to take place in the kinematics of the arm and hand segments. Very high acceleration values of up to 1471 G's are reported. At the same time, there are no contacts allowed for these segments with any of the vehicle components (a cost reducing decision for this initial simulation). Rapid oscillatory motions are observed for the lightweight hand masses. These unrealistic motions are of a high enough frequency to require a much smaller integration time step size than has been used in this simulation. The effects of these high G-level oscillations are reflected through the arm segments and perhaps even into the middle torso. This behavior often has caused problems with GMCVS (CVS, CAL3D, ATB) simulations, and specifically with steering column simulations reported in Reference 1. The solution was the addition of non-zero damping to the joint property definitions. An alternative solution, used by AMRL (12,13) in their recent rollover simulation of a restrained occupant, was to eliminate the small mass hands from the occupant definition, and also, to add damping at the joint structures.

Figures 16-21 show side views of the driver seated in the vehicle at 50-millisecond intervals during the crash event. These views assume that the location of the camera is fixed in vehicle coordinates. A normal seated position is assumed for time=0 milliseconds. At 50 milliseconds the occupant has sunk into the seat (or the seat has rotated up to push on the occupant) as the vehicle begins to roll. This can be observed by observing that the lower torso, upper legs, and feet penetrate the seat and floor more at 50 milliseconds than they do at 0 milliseconds. At 100 and 150 milliseconds the driver is observed to rise in the seat as a reaction to the initial forces and freefall during the time period before the vehicle contacts the ground. The driver appears to float more or less freely in the vehicle during the period from 200 through 300 milliseconds.

Two contacts that are initiated at about 350 milliseconds should be noted. These are left foot (LF) to the knee bolster (BOLSTERD) and upper legs (LUL and RUL) to the steering wheel rim (STEERINGWHEEL). These interactions were not included in the initial set of allowed contacts and, hence, do not generate contact forces. Both the dragging of the foot on the surfaces associated with the bolster region and contact of the legs and lap with the steering wheel rim and column should be included in more detailed simulations of unrestrained driver interactions with the vehicle interior during a rollover.

Many more interactions can be observed at 400 and 450 milliseconds. These include:

- Lower legs (LLL and RLL) to middle instrument panel (MIDDLEDASH)
- Upper legs (RUL and LUL) to the windshield (WINDSHIELD)
- Hands (LH and RH), lower arms (LLA and RLA), and upper arms (LUA and RUA) to the roof (ROOF)
- Head (H) to roof (ROOF)

The upper leg and head interactions are included and yield forces listed in Table 11. The other body segments pass through the vehicle interior surfaces. The initial objective of containment is achieved. The further objective of realistic and correct detailed kinematic and dynamic response can now be addressed in future simulations. The final graphic display at 500 milliseconds shows the containment of the five principal body segments with the remainder of the arms and legs outside the vehicle.

Figures 22 and 23 show a view of the Y-Z plane looking from the rear of the vehicle along the X-axis toward the front. At time=0 milliseconds, the driver is on the left side of the vehicle. The linear velocity of the vehicle is toward the right side of the view. As the vehicle begins to rotate, the occupant continues along the linear trajectory toward the passenger side. Following this trajectory places the occupant in contact with the roof by 450 milliseconds into the run.

Figures 24, 25, and 26 are tracings made from the dolly drop test films on which this simulation is based. They give an approximation of the kinematics shown in Figures 22 and 23. The camera that views the driver appears to be behind the passenger of the vehicle. It is aimed toward the initial position of the driver. As in the previous sequence, the driver slides across the seat and rises. At the final point in this movie sequence, the head and right shoulder appear to be interacting with the roof and the knees are at, or above, the level of the top of the instrument panel. Although it is not possible to analyze these test films quantitatively due to a lack of any calibration information, this qualitative review provides initial support for the capabilities of the GMCVS to simulate the complex dynamics of an unrestrained occupant during a complex rollover crash. Comparisons beyond about 500 milliseconds would not be too useful because of the interactions of the driver with the passenger dummy.

These results can also be compared with those from the MVMA 2-D simulations (4,5). It was found that the two-dimensional simulation results were unrealistic unless vertical knee motion was restricted. In other words, the two-dimensional case was limited to sliding of the occupant from one side of the vehicle to the other which somewhat resembled the kinematics observed in the film, even taking into account the presence of a passenger dummy. However, the possibility of the dummy rising off the seat with the knees at the level of the top of the instrument panel, as was observed in the movie and in the GMCVS output, was not possible with the two-dimensional simulation. The GMCVS can be expected to produce much more realistic results when the complete set of interactions among legs, arms, and vehicle interior are activated.



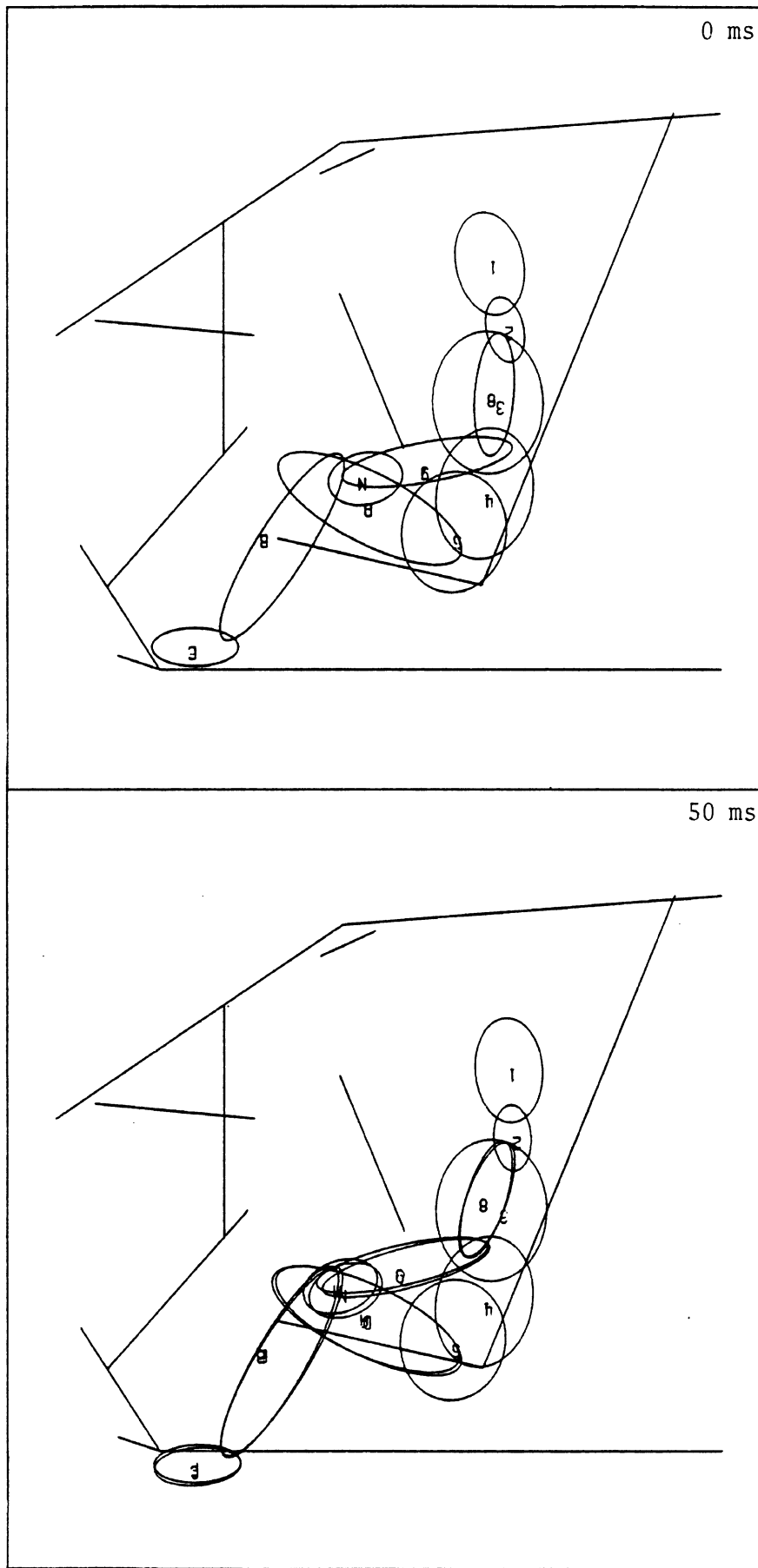


FIGURE 16. Side view of X-Z plane. 0 and 50 milliseconds.

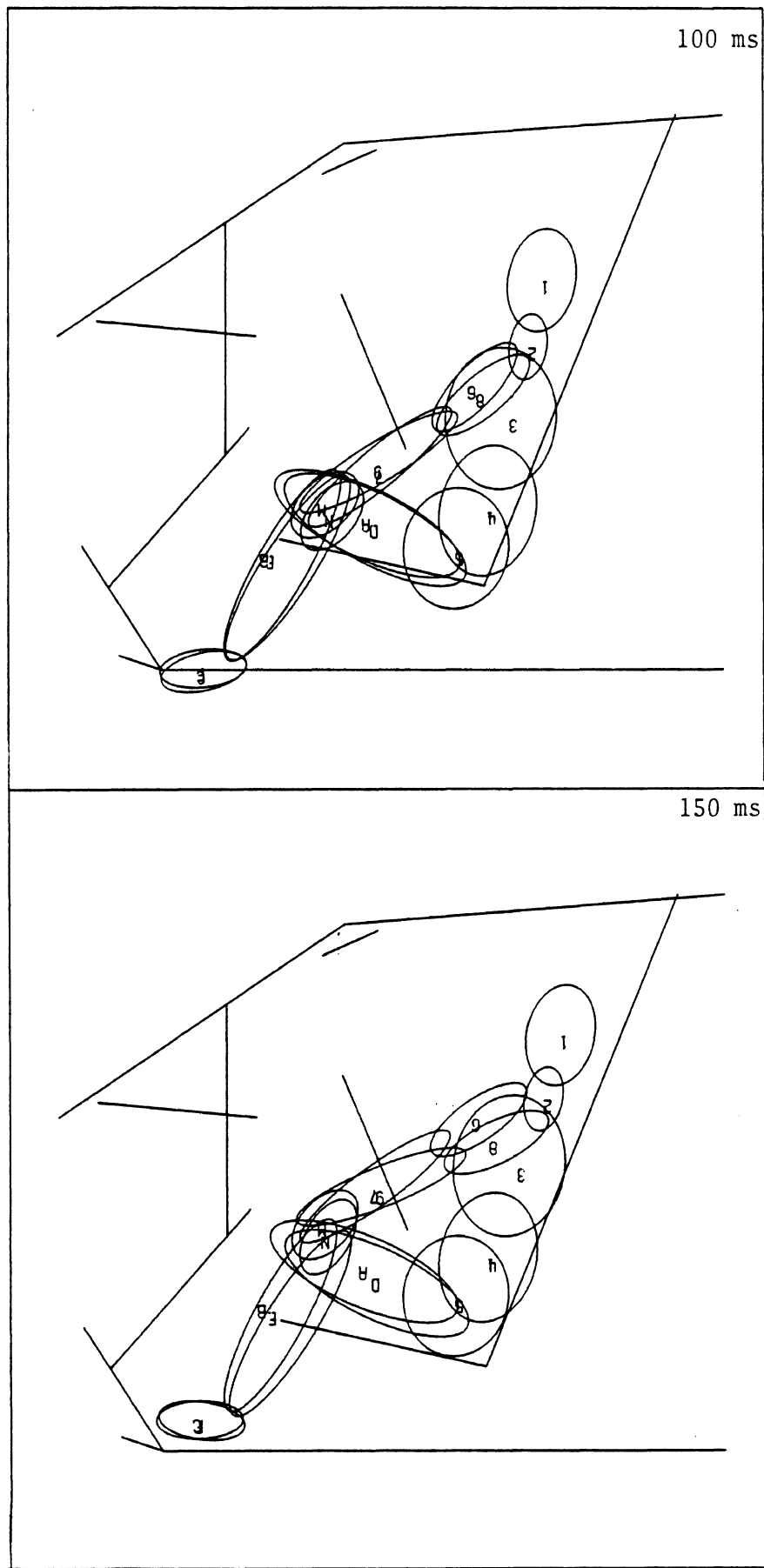


FIGURE 17. Side view of X-Z plane. 100 and 150 milliseconds.

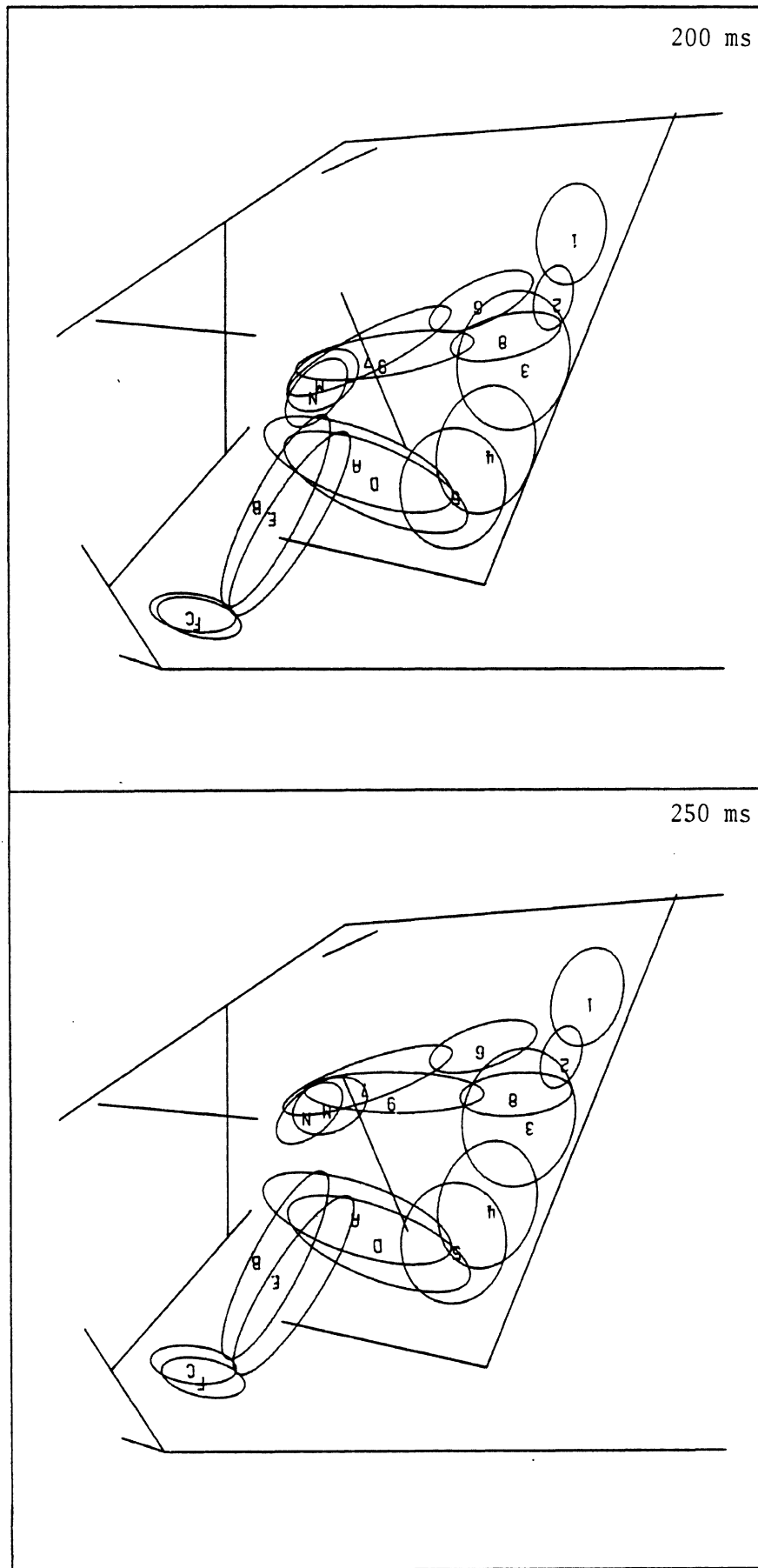


FIGURE 18. Side view of X-Z plane. 200 and 250 milliseconds.

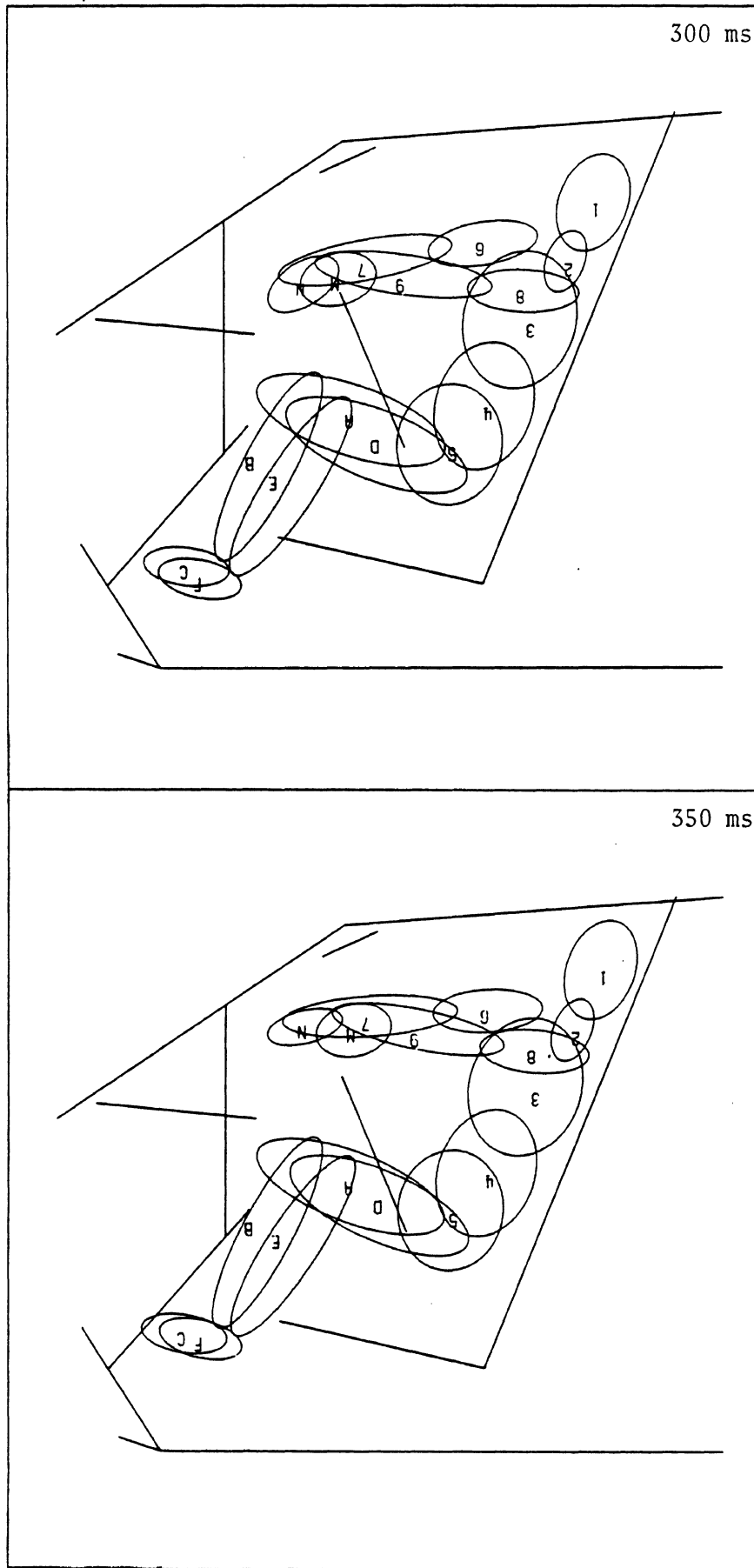


FIGURE 19. Side view of X-Z plane. 300 and 350 milliseconds.

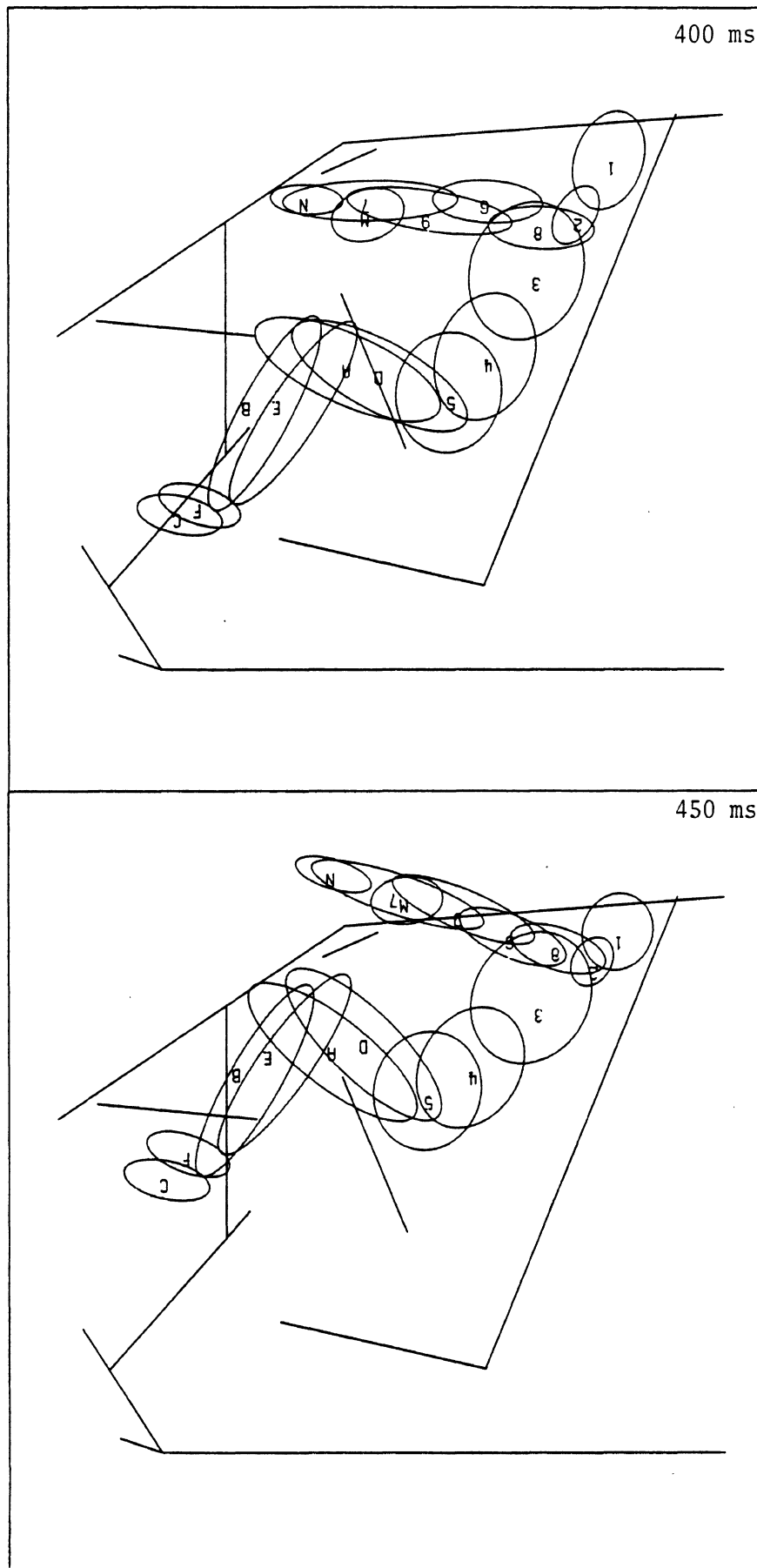


FIGURE 20. Side view of X-Z plane. 400 and 450 milliseconds.

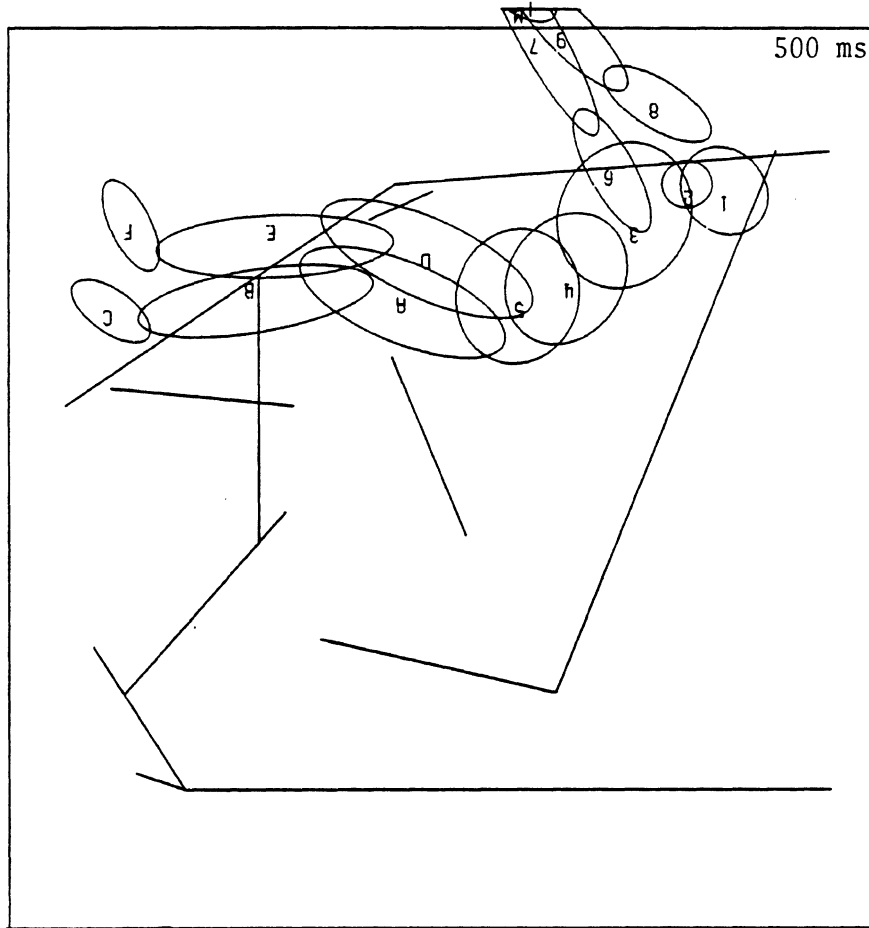


FIGURE 21. Side view of X-Z plane. 500 milliseconds.

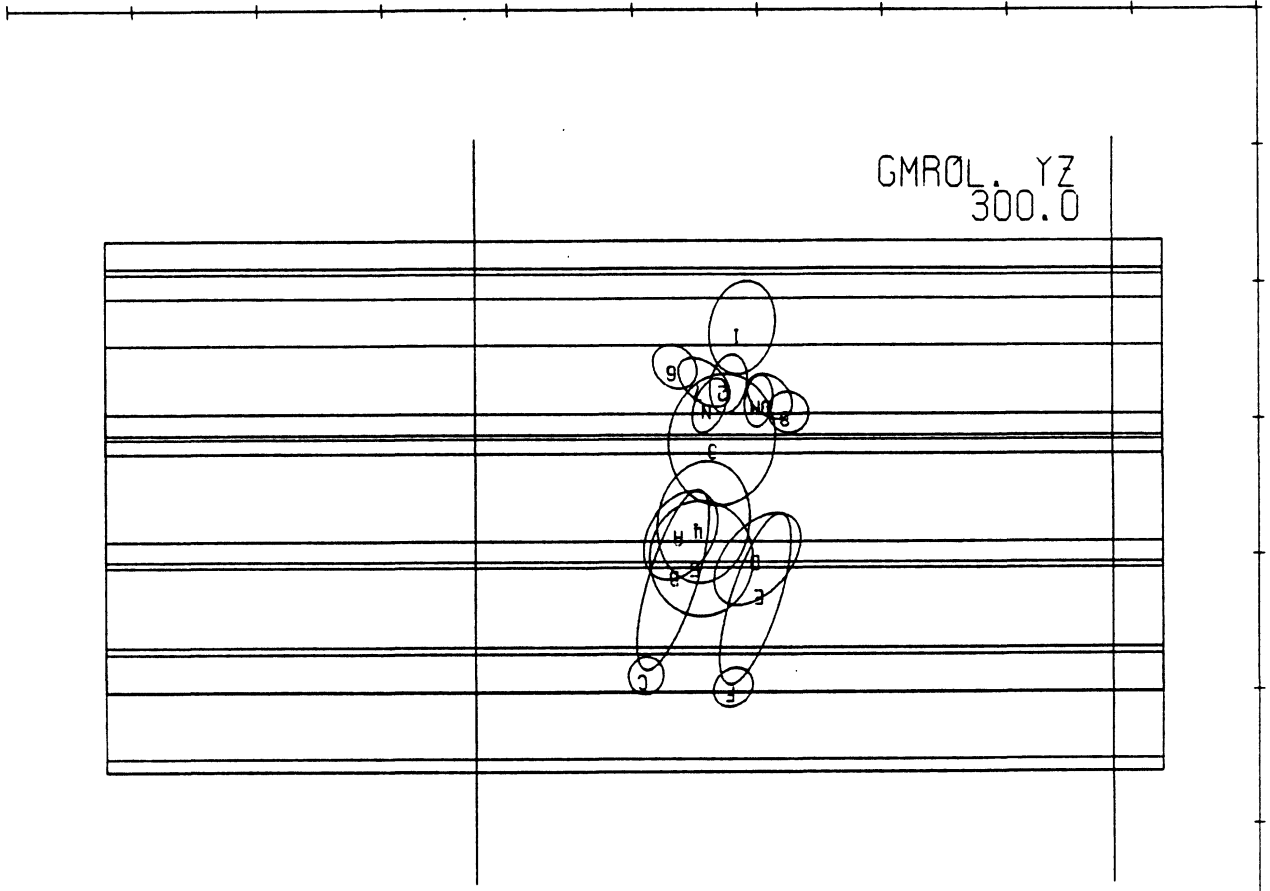
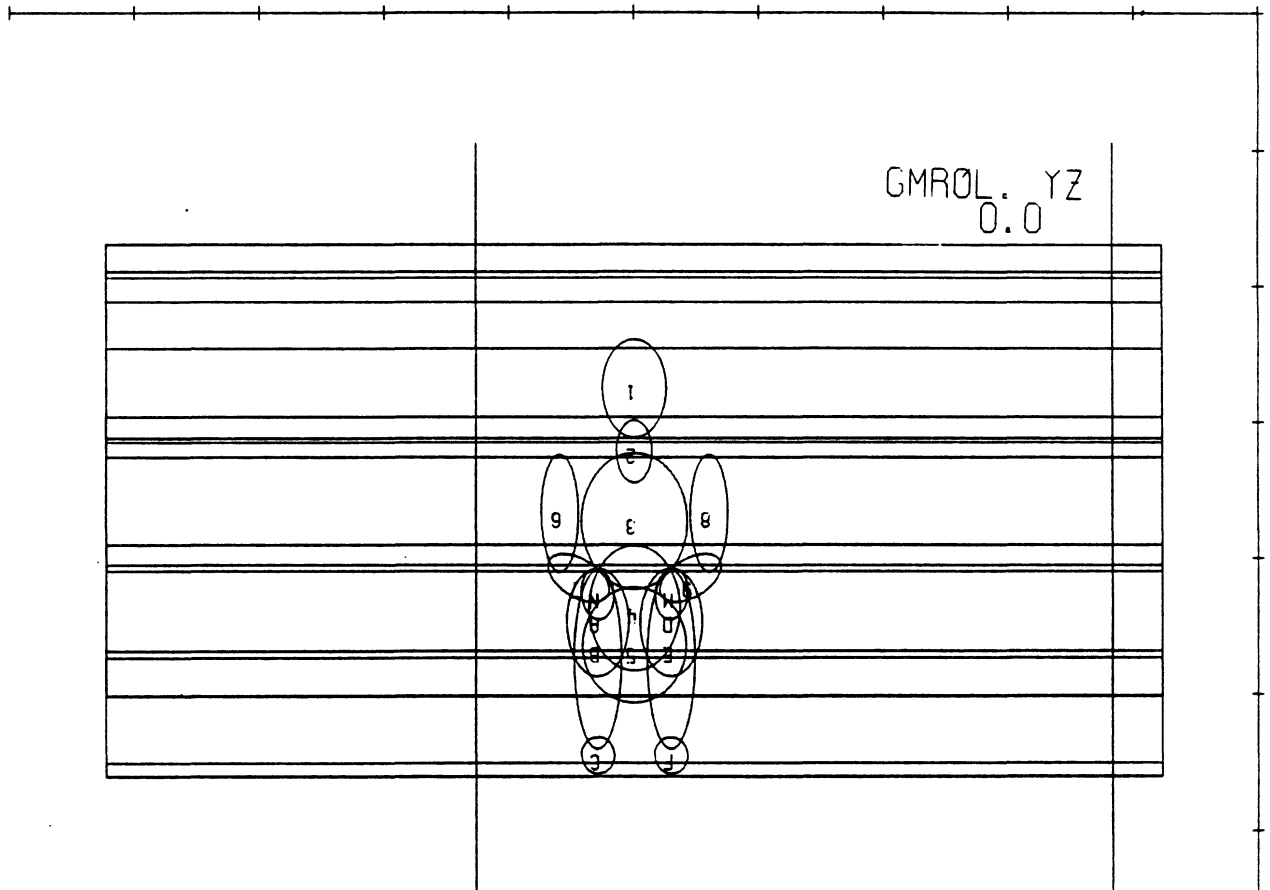


FIGURE 22. View from back of Y-Z plane. 0 and 300 milliseconds.

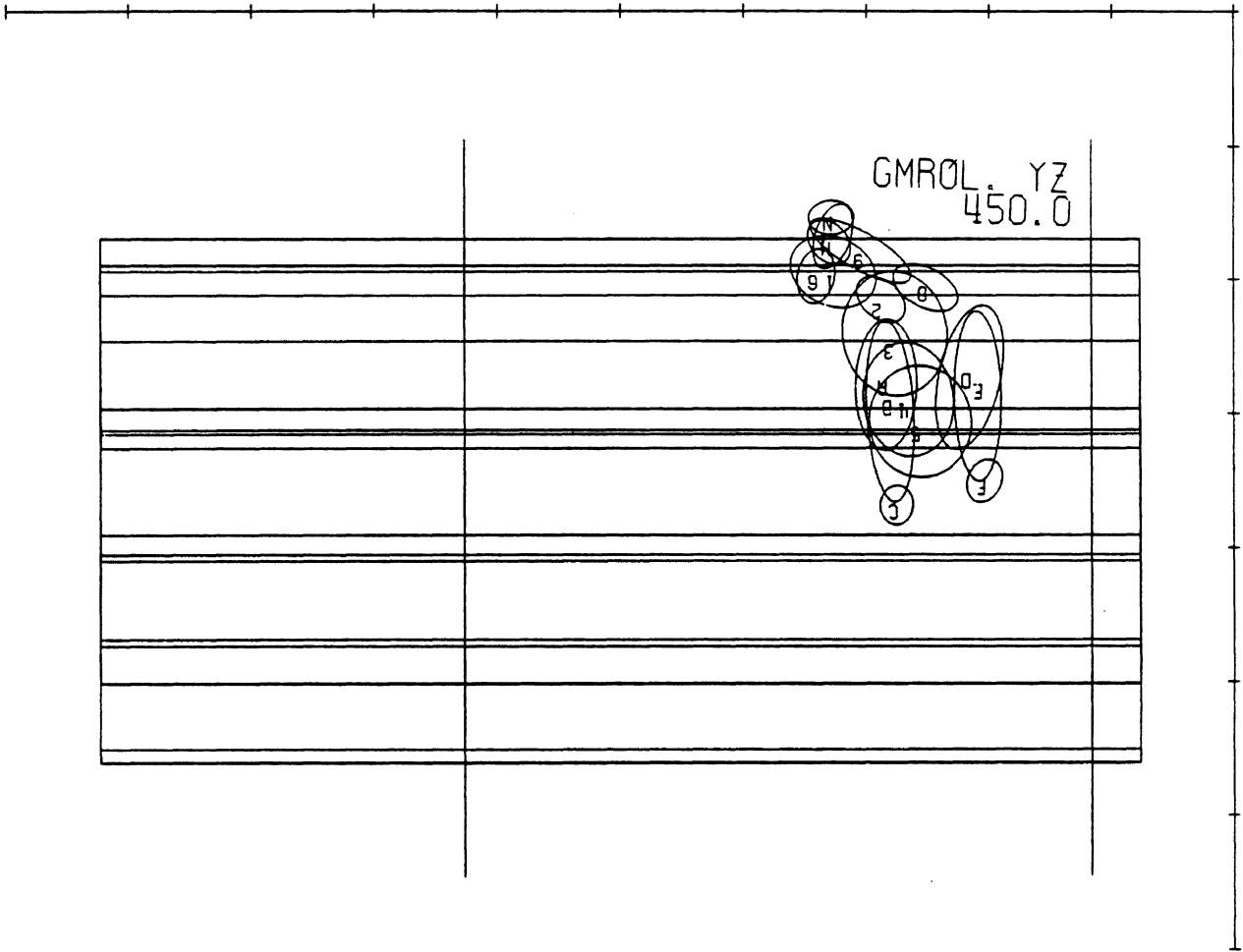


FIGURE 23. View from back of Y-Z plane. 450 milliseconds.



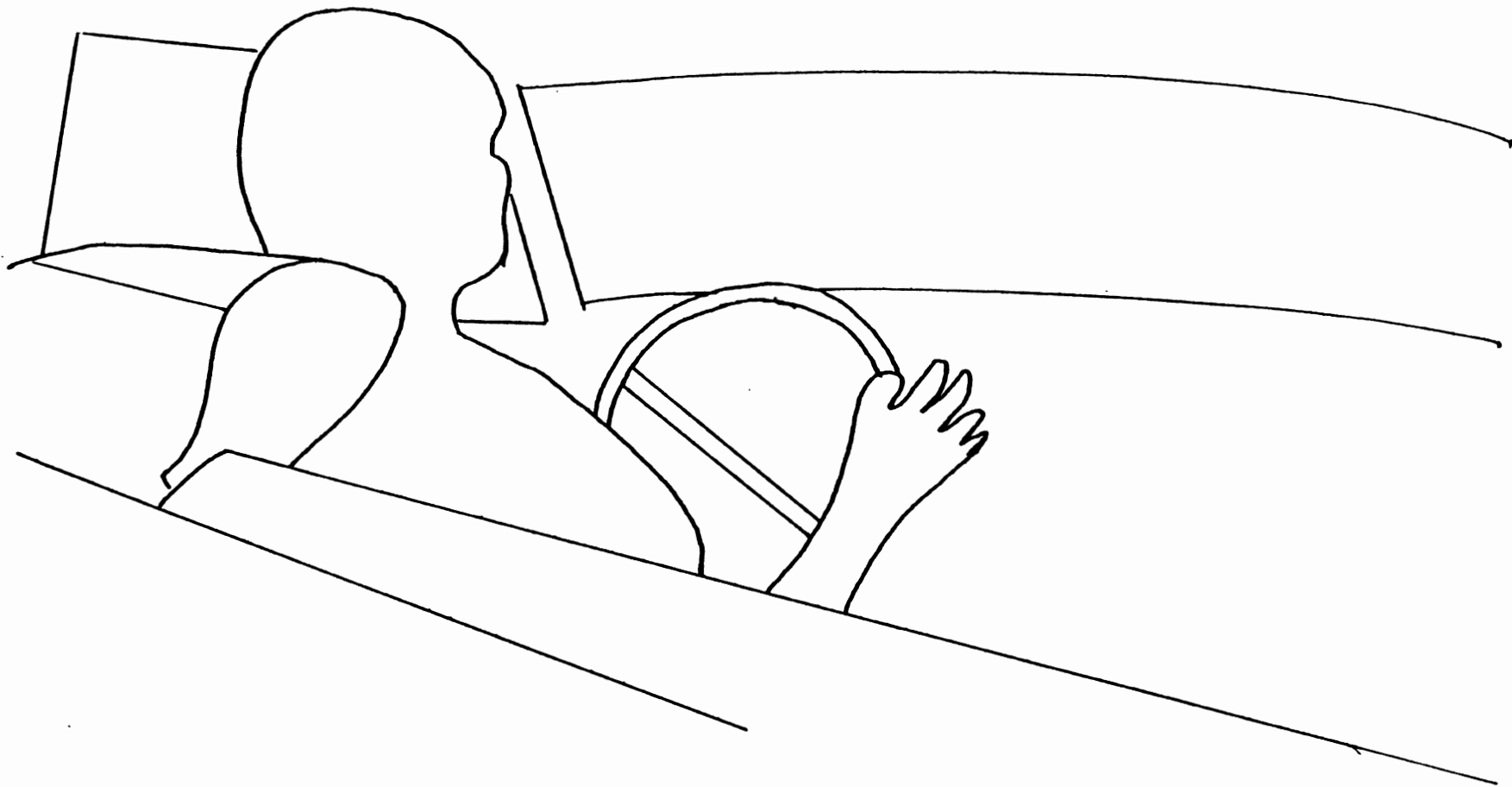


FIGURE 24. Tracing of driver from rear seat camera view. 0 milliseconds.

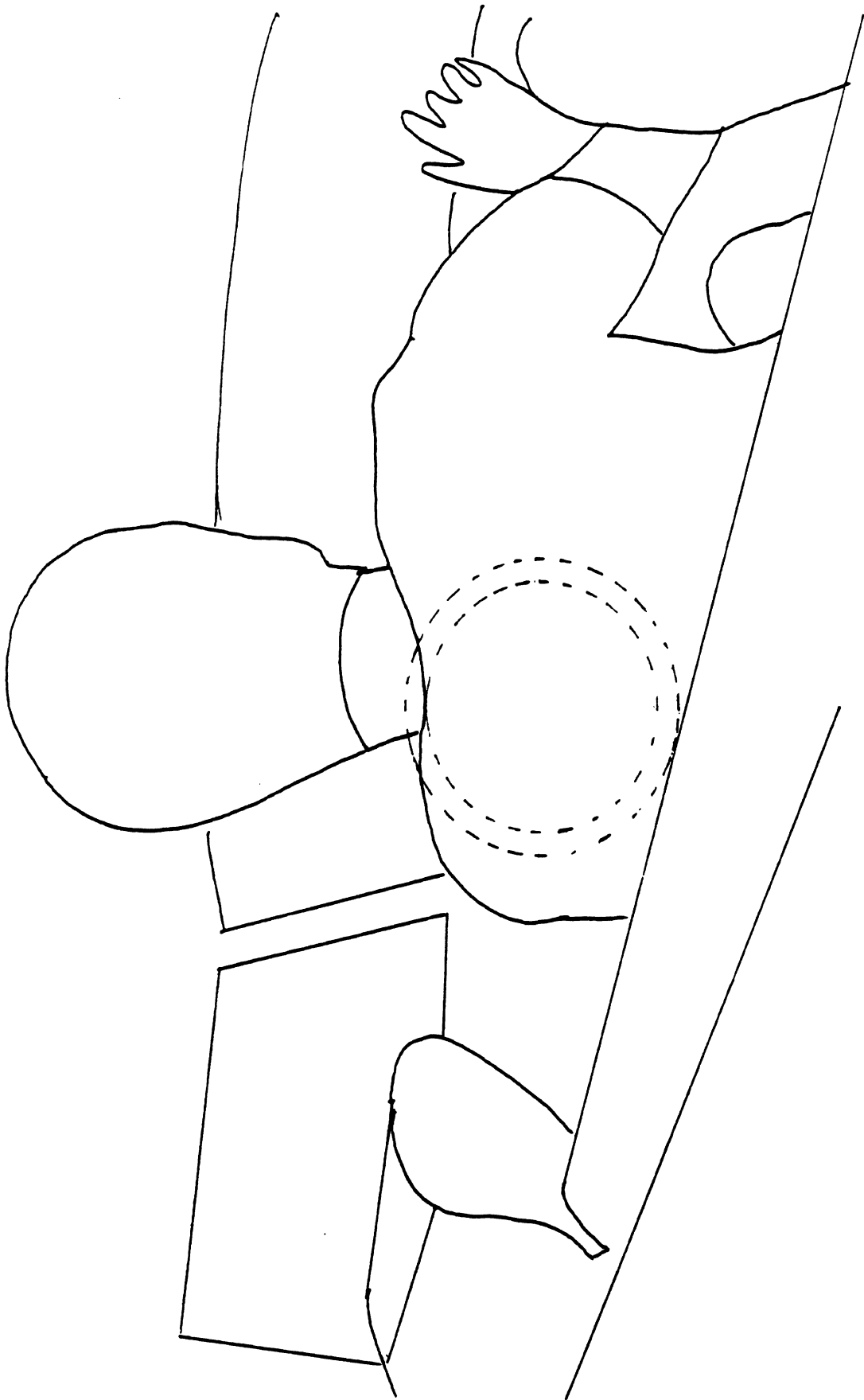


FIGURE 25. Tracing of driver from rear seat camera view. ~250 milliseconds.

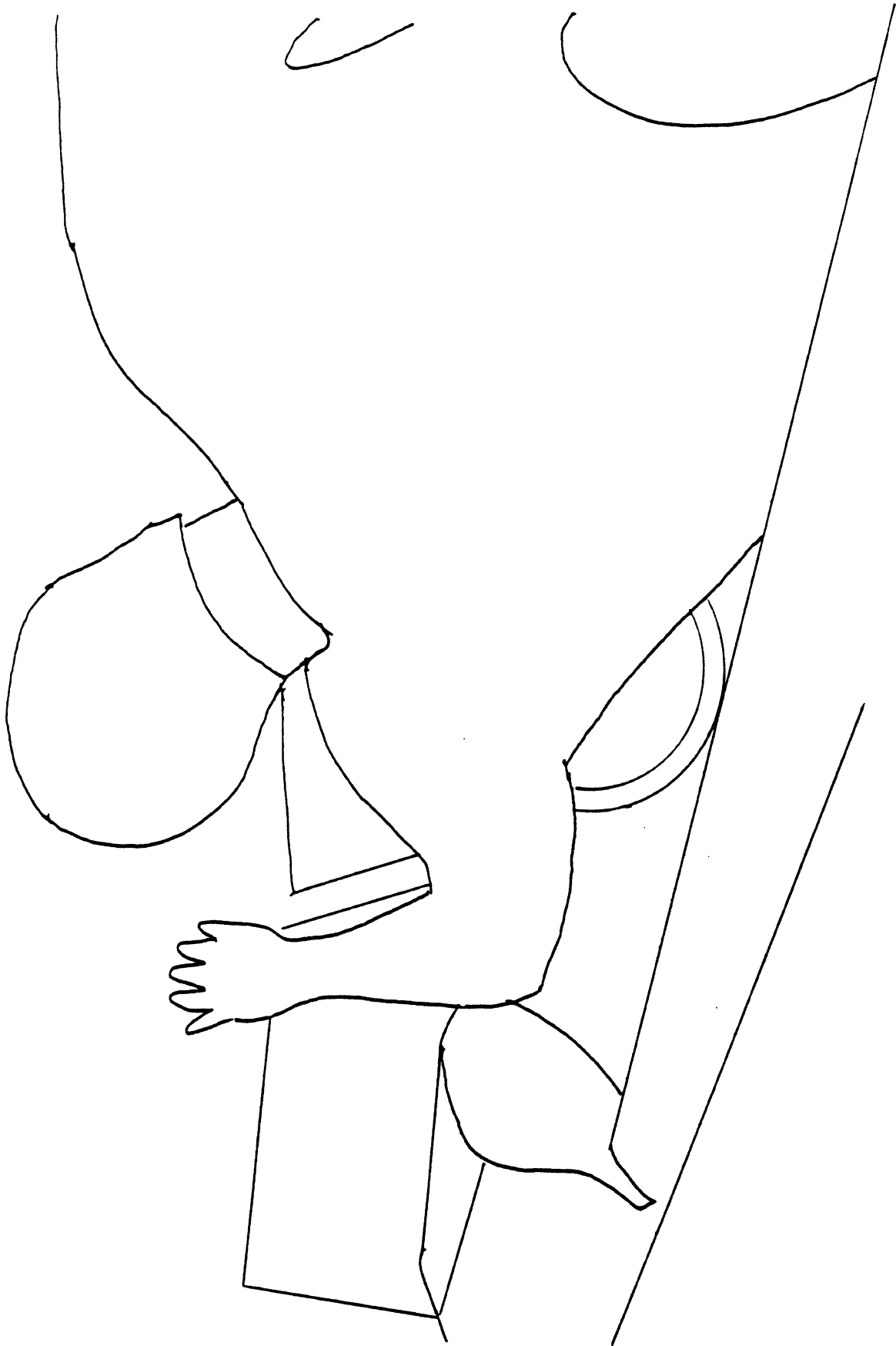


FIGURE 26. Tracing of driver from rear seat camera view. ~500 milliseconds.

## 4.5 CONCLUSIONS AND RECOMMENDATIONS

The following is a list of conclusions and recommendations based on the initial full-scale rollover simulation.

1. An initial full-scale simulation has been made that demonstrates the capabilities of the GMCVS for modeling complex rollover events.

2. A primary criterion for the selection of appropriate contact interactions between the occupant and the vehicle is to initially choose those that appear to be the most critical to overall containment of the occupant inside the vehicle (unless ejection is the subject of the simulation).

3. Great care must be taken in setting up vehicle motion input due to spline-fit code sensitivity to the shape of the position versus time curves in the neighborhood of time = 0 milliseconds.

4. Rapid oscillatory motions were observed for light weight masses, particularly the hands. This phenomenon can lead to solution instability. The proposed solutions are addition of damping to the joints used in the Hybrid III data set or elimination of the hand masses from the model.

5. The simulated occupant kinematics were qualitatively similar to those obtained from review of films taken of the original dolly drop rollover test. The occupant appeared to move and interact with the vehicle interior properly.

## 5.0 GUIDELINES FOR THE LAYOUT OF GMCVS SEGMENT DATA

The GMCVS model can be used to simulate any situation which can be represented with one or more linkages and with one or more prescribed coordinate systems. These guidelines provide methods for the user that deal with the general problems of specifying segments and linkages of segments for input to the GMCVS model.

The GMCVS model is primarily used to simulate vehicle occupant motion during a crash situation. The occupant is represented by a linkage of rigid segments with ellipsoids attached to sense contact with the vehicle. The vehicle is most often represented by a coordinate system for which motion is completely prescribed in the input data set. Parallelogram-shaped planar surfaces, attached to the vehicle, sense contact with the occupant.

A terminology for description of the general problem is first presented. The rules of GMCVS model input data organization are then discussed, making use of this terminology. A brief description of GMCVS model input data cards is presented to the extent which they affect the layout of GMCVS segment data. Finally, development of four example data sets is described from problem description to GMCVS data deck layout.

### 5.1 GENERAL TERMINOLOGY AND DEFINITIONS

This section presents the necessary terminology to describe any configuration which the GMCVS model is able to simulate. The scope of this section is the description of the geometric structure, not the specification of all physical properties.

**5.1.1 Segments.** The fundamental concept in the GMCVS model data description is "segment." A segment is defined as a coordinate system which may be (and usually is) associated with a rigid body. If the association between the coordinate system and the rigid body exists, the center of gravity of the rigid body is coincident with the origin of the coordinate system and the orientation of the principal axes of the rigid body is fixed with respect to the axes of the coordinate system. This coordinate system is considered to be the "local geometric axes of the segment." Each segment has six degrees of freedom associated with it for general considerations. A segment not associated with a rigid body is a reference system and is called a "massless" or "imaginary" segment. All vehicles with prescribed kinematics are of this type. Figure 27 illustrates a typical segment associated with a rigid body.

**5.1.2 Connections.** A "connection" between two segments is defined as any fixed relationship between degrees of freedom associated with the two segments. Connections include, for example, a ball and socket joint at specified points in the two segments, and roll/slide constraints between two segments along their boundaries. Many other types of connections exist. Let us define an "explicit" connection to be a fixed joint at a prescribed point in both segments and an "implicit" connection to be a variable constraint. In what follows, connection will mean explicit connection unless otherwise stated.

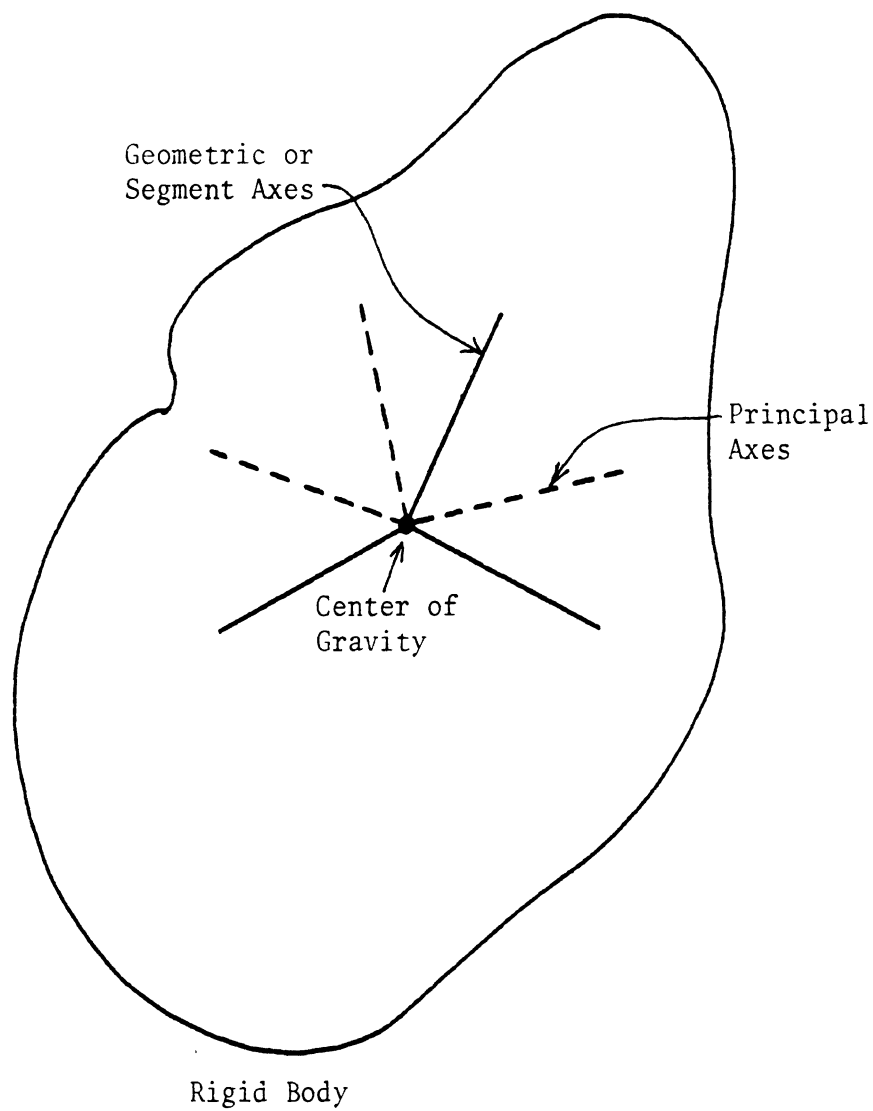


FIGURE 27. Typical segment.

**5.1.3 Chains and Links.** A "chain" is either a single unconnected segment or any group of segments for which an unbroken path of segments and connections can be found between any two of the segments. A "link" is any segment which is an element of a chain. The "base link" of a chain is the single link of the chain for which the linear positional coordinates are taken as degrees of freedom. While any link of a chain can be chosen for this, not all choices are equally efficient. In most cases, one of the heavier and more centrally located links should be chosen. Such a choice will yield a more numerically stable solution. The linear positional coordinates of all other links of the chain will be determined from:

- the linear coordinates of the base link,
- the locations of the connections, and
- the angular degrees of freedom of all the links of the chain on the path from the base link to the segment.

**5.1.4 Branches.** Any link in a chain with exactly two connections is called an "internal" link. Any link in a chain with either one connection or more than two connections is called an "end" link. A "branch" is a set of contiguous links which begins with an end link, has zero or more internal links, and ends with another end link. The branch which contains the base link is called the "main branch." Since the base link may belong to more than one branch, the main branch is usually selected to have the maximum number of connections and the maximum mass.

The end link of any branch which forms part of the path from the branch back to the main branch is called the "branch base link." Any branch A is said to be "dependent" upon another branch B when branch B makes up part of the path from branch A back to the main branch. All branches which are directly dependent on the main branch (i.e., for which either end link of the main branch serves as branch base link) belong to level two and are called "secondary" branches. Tertiary branches (level three) are those branches which are directly dependent upon secondary branches. Higher levels are similarly defined. In general, every link with N connections where N is greater than two will belong to exactly N branches. N-1 of these branches will belong to the same level and are dependent upon the Nth branch which belongs to one level below the rest. Every link with just one or two connections will belong to exactly one branch.

Figure 28 illustrates a simple chain constructed of three branches. Link 1 is here taken as the base link. Any of the three branches fit the definition of main branch with link 1 then serving as branch base link for both the other two branches. Assume that the branch composed of link 1, link B2, and link B3 has the most mass and is taken to be main branch with the other two branches being the secondary branches.

**5.1.5 Uniqueness of Paths.** There must be only one path of links and connections (without repeating links) between any two links in a chain. This is equivalent to saying that no closed loops can exist in any chain. A corollary of this statement is that every branch base link must be unique once the chain base link and main branch are chosen. However, closed loops can be simulated by careful use of implicit connectors. Note that this fact does not violate the unique path rule because implicit connectors do not alter the structure of the chains involved.

**5.1.6 Preferred Order of Segments.** The following list of rules defines the preferred order of segments for defining a linkage for use with the GMCVS model. These rules embody some concepts of "neatness" which are not strictly necessary but which are recommended for developing easily readable data sets. It will be stated what part of each rule is necessary.

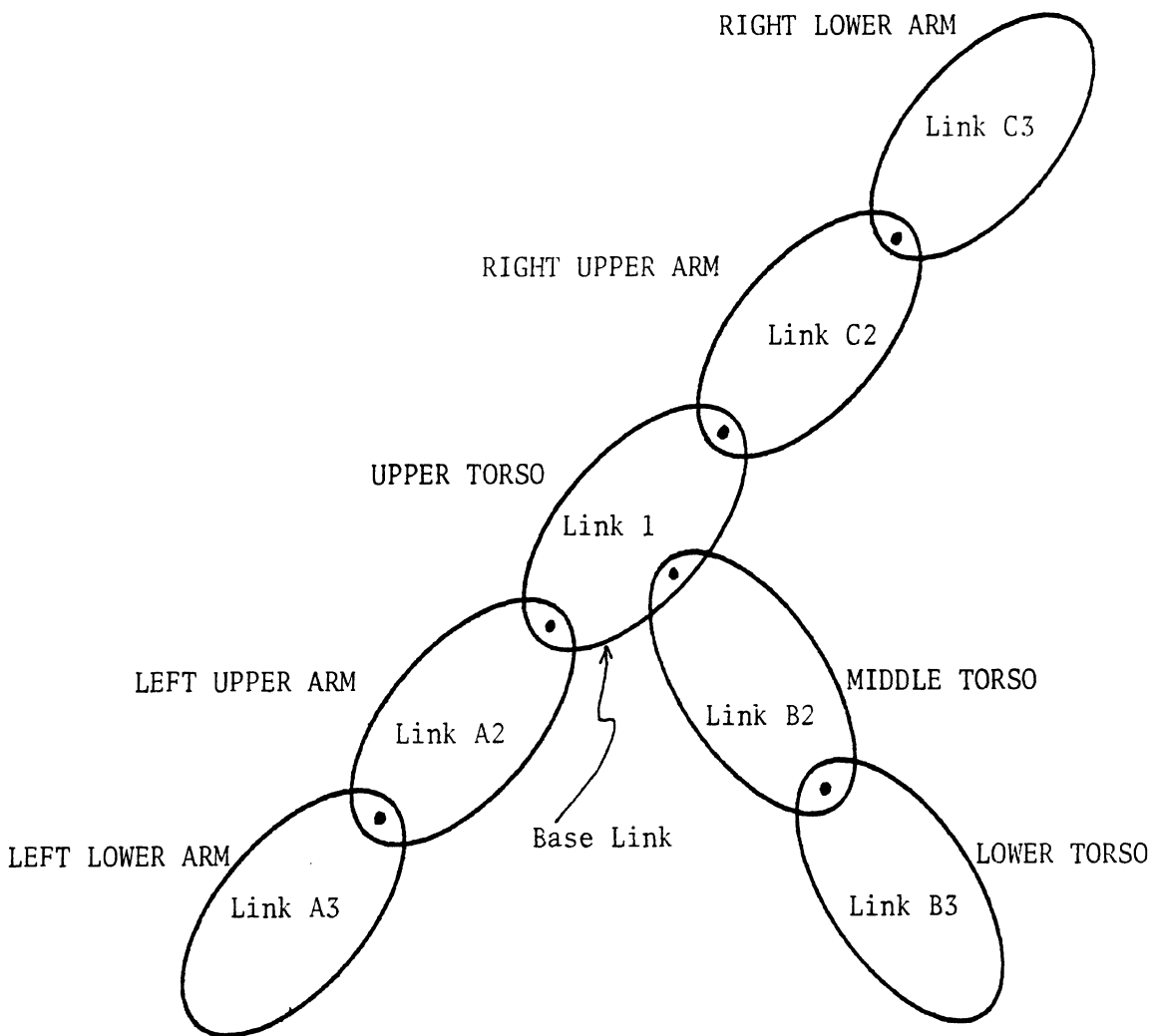


FIGURE 28. Three branches of three segments each forming one chain of seven segments.



1. All segments for each chain should be contiguous.
2. The base link for any chain must be the first segment of the chain.
3. The numbering of the rest of the segments defining the main branch should follow in outward order from the base link to the end link of the main branch in each direction. While it is not necessary to include both end links before including the branches dependent on the end link already included, it is usually advantageous to keep the main branch contiguous.
4. After the main branch is completely included, the secondary branches are included by starting with the link connected to the branch base link outward through the other end link contiguously.
5. After all secondary branches are included, then tertiary branches are included in a similar fashion. If only a few short tertiary branches exist, the user may chose to place them immediately after the secondary branches upon which they are dependent. This is a matter of personal preference.
6. It is necessary to keep all dependent paths in an order outward from the base link. The above rules will accomplish this; however, it is possible to relax these rules and intermix all dependent paths and all different chains as long as the order in every dependent path is maintained. It is strongly recommended that the user does not intermix paths and chains except with the greatest of caution and only when the advantages outweigh the increased confusion which will certainly result.

**5.1.7 An Unusual Twenty-One Segment Man.** Suppose that the torso is represented by three segments (upper, lower, middle), neck and head each by one segment, and the arms and legs each by three segments (upper, lower, extremity). Further, let the right fingers and left toes each be represented by two segments. Figure 29 illustrates this configuration.

It is clear that only one chain is present since a line of connections exists between any two of these segments. A natural choice of base link for this chain would be one of the torso elements. A logical choice is the lower torso because of the number of connections, the large mass, and the relation of the H-point to design specifications. The three torso elements form a branch since the upper torso (four connections) is one end link, the middle torso (two connections) is an internal link, and the lower torso (three connections) is the other end link. It is also clear that the arms, legs, and head-neck taken together with the connecting end link of the main branch, constitute all secondary branches. The following combinations of links constitute all tertiary branches:

- right hand and right thumb,
- right hand and right fingers,
- left foot and left big toe, and
- left foot and left toes.

These twenty-one segments can be ordered according to the rules of the last subsection starting with four different choices of base link. Table 13 lists these results.

It should be noted that the base link which is chosen does not affect branch constituency. Branches are included either in order or in reverse order. The middle torso column illustrates this using the alternative mentioned in rule five of Section 5.1. Neither head nor thumb are good choices.

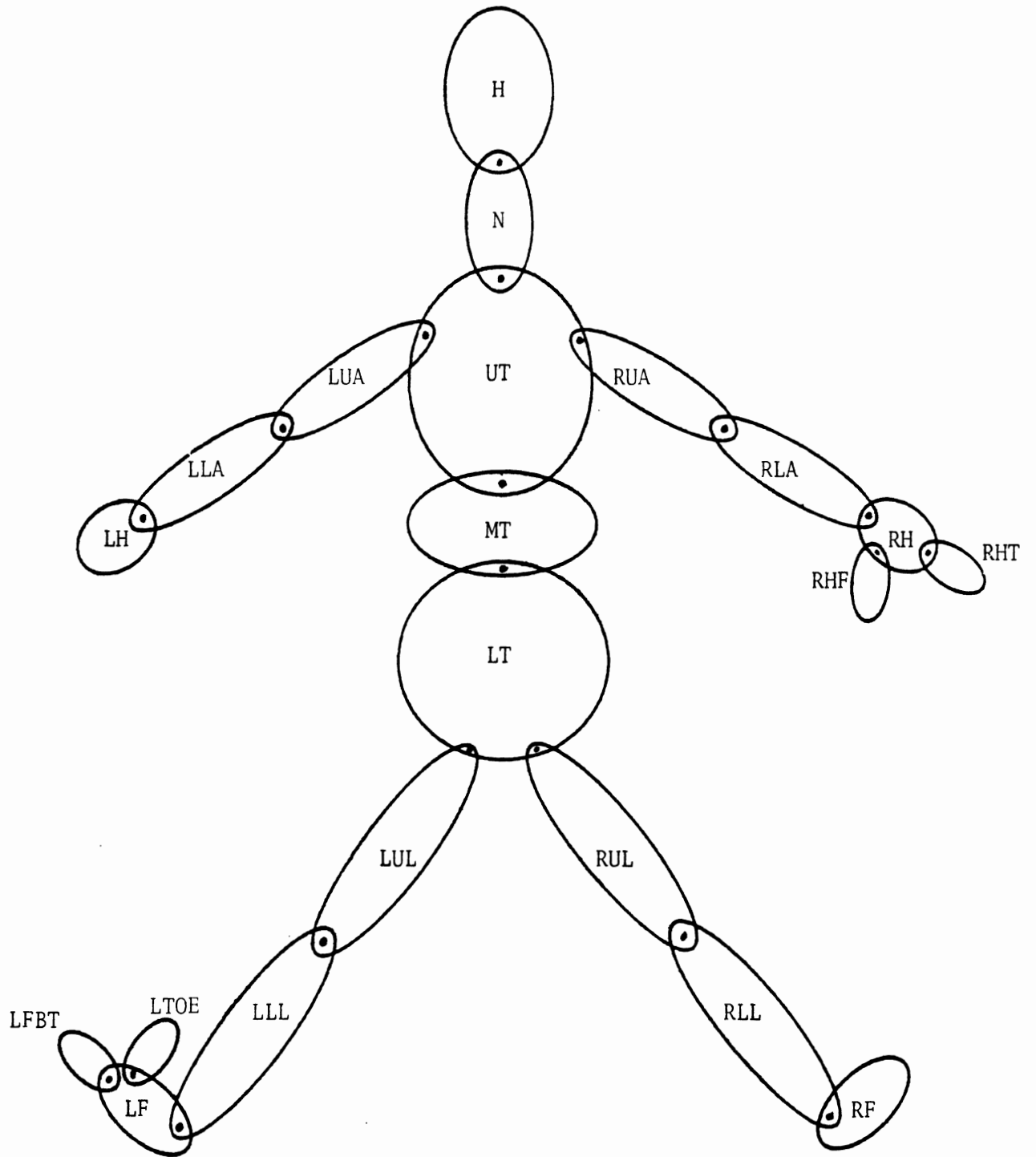


FIGURE 29. An unusual 21-segment man.

TABLE 13

## ORDER OF SEGMENTS AS A FUNCTION OF BASE LINK CHOICE

Segment Number	Upper Torso	Middle Torso	Head	Right Thumb
1	UT (upper torso)	MT	H	RHT
2	MT (middle torso)	LT	N	RH
3	LT (lower torso)	UT	UT	RHF
4	N (neck)	N	MT	RLA
5	H (head)	H	LT	RUA
6	RUA (right upper arm)	RUA	RUA	UT
7	RLA (right lower arm)	RLA	RLA	MT
8	RH (right hand)	RH	RH	LT
9	LUA (left upper arm)	RHT	LUA	N
10	LLA (left lower arm)	RHF	LLA	H
11	LH (left hand)	LUA	LH	LUA
12	RUL (right upper leg)	LLA	RUL	LLA
13	RLL (right lower leg)	LH	RLL	LH
14	RF (right foot)	RUL	RF	RUL
15	LUL (left upper leg)	RLL	LUL	RLL
16	LLL (left lower leg)	RF	LLL	RF
17	LF (left foot)	LUL	LF	LUL
18	LFBT (left big toe)	LLL	LFBT	LLL
19	LTOE (left toes)	LF	LTOE	LF
20	RHT (right thumb)	LFBT	RHT	LFBT
21	RHF (right fingers)	LTOE	RHF	LTOE

## 5.2 DESCRIPTION OF THE CVS INPUT DATA CARDS FOR SEGMENT DEFINITION

The GMCVS model depends upon exact card order in the specifications for any simulation. Although card identifications should be specified in the GMCVS input data description for all cards which do not have data in all eighty columns, these card identifications are ignored by the GMCVS model. It is highly recommended that card identifications be used to increase input data deck readability. There are cases for which data deck readability can be further enhanced by altering the prescribed card identification. These cases will be discussed for the individual data cards. The identification fields of data cards can be used as the user sees fit.

The remaining subsections discuss data cards of the GMCVS model which have an impact on the geometric structure to be simulated. This presentation assumes the user has access to a copy of the GMCVS model input data description and is supplementary to it.

**5.2.1 Segment Cards (B.2).** Segments associated with rigid bodies and some of the massless segments are specified by means of B.2 cards. There are NSEG such cards where NSEG is specified on card B.1. The order of B.2 cards determines the order of the segments which they describe. The card identifications for segments are B.2.A through B.2.Z can be located in columns 73 through 80 as needed. Data deck readability would be increased if these were replaced by B.2.01 through B.2.99. Each segment card would then contain the segment number. It would still be necessary to maintain correct card order since that is how the GMCVS code actually orders segments.

The GMCVS model expects that each segment specified will have at least one contact-sensing ellipsoid attached to it. This ellipsoid will be used to produce forces if, and only if, interactions are specified for it on the appropriate F cards.

**5.2.2 Joint Cards (B.3-B.5).** All explicit connections are specified by use of these cards. There are NJNT sets of each of these cards where NJNT is specified on card B.1. NJNT is usually NSEG-1, but may be NVEH-1 or NGRND-1 if it is desired to explicitly connect a chain to one of the vehicles or to the ground system (inertial system). NVEH, the segment number associated with the vehicle, is defined in the next subsection. NGRND, the segment number associated with the inertial coordinate system, is defined as NVEH+NBAG+1 where NBAG is specified on card D.1 as the number of airbags. In every case, the Jth joint connects segment JNT to segment J+1 where JNT is specified on card B.3. The quantity JNT must be either zero or a number less than J+1 in magnitude. Segment one and any segment N for which the JNT of joint N-1 is zero is a base link of a chain. It is possible to joint any base link to a vehicle or the ground in which case the effective base link of the chain would become the vehicle or the ground and rule two of Section 5.1.6 would not apply.

The prescribed card identification could advantageously be modified in a manner similar to the last subsection to explicitly include a two-digit joint number instead of a letter.

**5.2.3 Vehicle Specifications (C.1-C.5).** Massless segments, whose degrees of freedom are completely prescribed by input data cards, are termed vehicles in the GMCVS model. At least one, and up to six, such segments must be specified by use of C cards. The optional segments are called secondary vehicles and may be specified to either be coincident with a massless base link among the first NSEG segments or may be specified as an additional segment. In the latter case, the first such vehicle must be numbered

NSEG+1, the second such vehicle must be numbered NSEG+2, and so on. The vehicle which is always required is called the primary vehicle and is assigned the next number after the last of the secondary vehicles which are numbered greater than NSEG (this number is given the name NVEH).

**5.2.4 Contact Surface Cards (D.2).** Parallelogram-shaped planar contact-sensing surfaces can be specified by means of D.2 cards. There are NPL such sets of cards where NPL is specified on card D.1. Usually these contact planes are attached to one of the vehicles or the ground, but can be attached to segments numbered less than NSEG+1. These attachments are specified by use of F.1 cards.

**5.2.5 Ellipsoid Cards (D.5).** Additional contact sensing ellipsoids are specified with D.5 cards. There may be NELP such sets of cards where NELP is specified on card D.1. These additional ellipsoids may either take the place of ellipsoids specified on B.2 cards, in which case they are numbered less than NSEG+1, or be added to the existing ones, in which case they are numbered greater than NGRND-1. The axes of all ellipsoids specified on B.2 cards are assumed parallel to the segment axes, whereas all ellipsoids specified on D.5 cards may be rotated by specification of orientation angles in the data set.

**5.2.6 Interaction Specifications and Roll Constraints (F.1 and F.3).** F cards have several functions. First, they specify which ellipsoids are allowed to contact other ellipsoids and contact planes. Second, they specify which ellipsoids and contact planes are attached to which segments. Third, they specify what material properties are associated with each of the specified interactions. Among the options for interactions are roll-slide constraints. Here again, the details of setting up the data cards which specify material properties and constraints are topics for another guideline.

The card identifications for F.1 and F.3 could also be modified in a manner similar to the previous subsections, except the two-digit numbering might be assigned "00."

**5.2.7 Segment Constraints (D.6).** Three other types of implicit connections can be specified with D.6 cards. There are NQ such sets of cards where NQ is specified on card D.1. These connections are defined as follows:

- an arbitrary point in one segment is constrained to be coincident with an arbitrary point in another segment,
- an arbitrary point in one segment is constrained to be a fixed non-zero distance from an arbitrary point in another segment, and
- a tension element constraint connects arbitrary points in two segments.

While the first of these constraints is logically equivalent to the definition of an explicit connection given in Section 2.2, the functional characteristics of this constraint lead to its classification as an implicit connection. The user should not use constraints for normal chain-building.

**5.2.8 Segment Kinematics Output Control Cards (H.1-H.6).** The GMCVS model allows the user to specify the points on segments for which either linear and/or angular accelerations, velocities, and/or displacements are desired. The GMCVS model automatically prints segment accelerations in local coordinates (directly related to A-P and S-I). Segment velocities and displacements are printed with respect to the primary vehicle system. The implications of this are that the user may choose to use the primary vehicle purely as an output reference system while using one of the secondary vehicles to drive the simulation. The GUCVS Version of the CVS Model allows the user to specify what output frame of reference is desired for each individual kinematic output.

### 5.3 FOUR RELATED EXAMPLES

Each of the following four subsections start with the description of a given linkage model, continues with the layout of segments, joints, constraints, ellipsoids, contact planes, and vehicles used, and finally discusses the selection, number, and order of input data cards which will be needed.

**5.3.1 Vehicle Crash with Occupant, Column Mass, and Wheel Mass.** The first model is an occupant positioned to impact the steering column and wheel when the vehicle crashes. Gross interaction of the occupant with the steering wheel is the object. Output kinematics relative to the vehicle are desired.

To achieve these ends, the occupant will be represented by three segments. The vehicle will be represented by the primary vehicle with two additional segments jointed to it for the steering column/wheel. The rest of the passenger compartment is represented by use of contact planes attached to the vehicle. Another contact plane is attached to the steering wheel segment. An acceleration profile for the primary vehicle describes the crash situation.

Figure 30 illustrates this crash. In this and the following figures, the one to four character names printed within the segment outlines are the GMCVS segment names required on the B.2 cards. The one to twenty character name near each contact plane is the description required for planes on D.2 cards.

Table 14 summarizes the segment information. Table 15 summarizes the joint information. Table 16 summarizes the contact plane information. Table 17 summarizes the allowable interaction specifications.

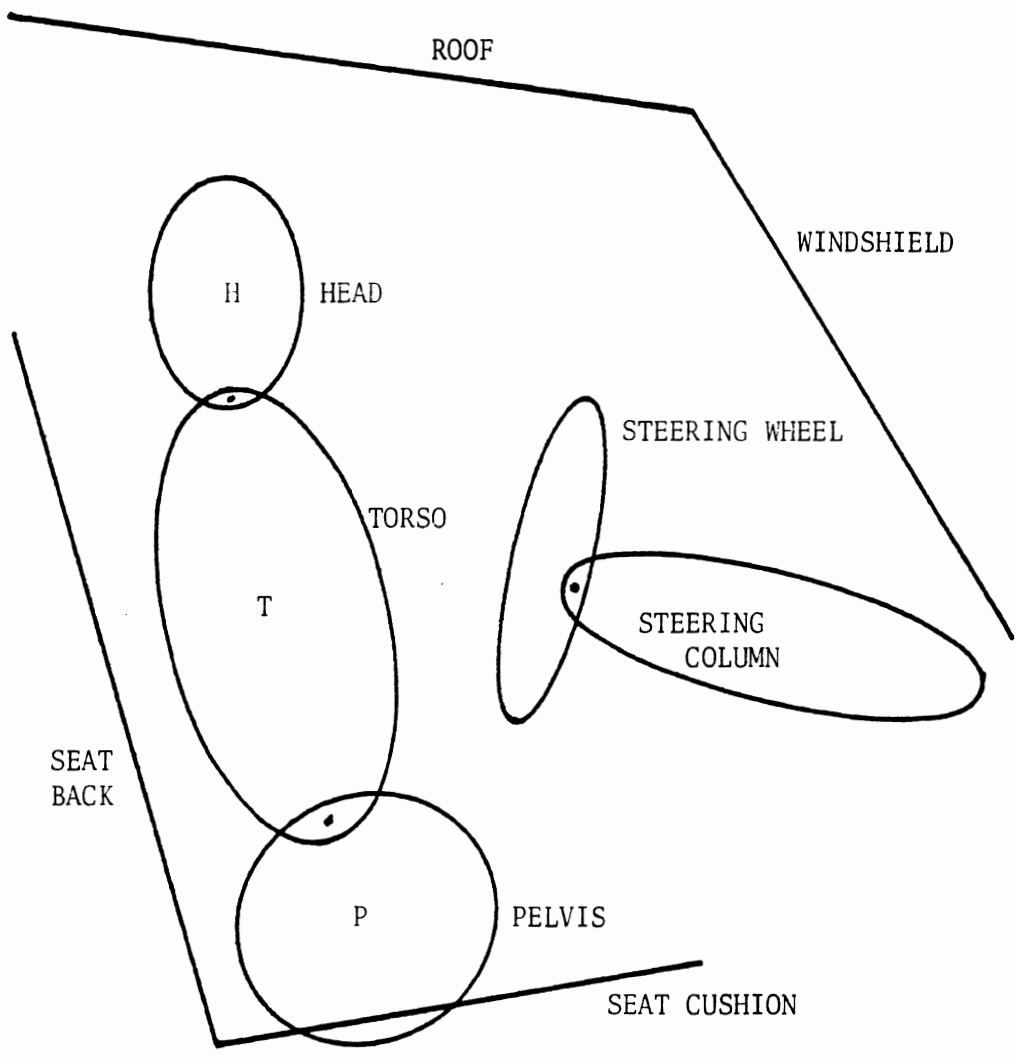


FIGURE 30. Three-segment man in vehicle with two attached segments.

TABLE 14  
B.2 CARD INFORMATION WITH NSEG=5

LAST ID	SEG	DESCRIPTION
01	T	TORSO OF OCCUPANT
02	P	PELVIS OF OCCUPANT
03	H	HEAD OF OCCUPANT
04	COL	STEERING COLUMN
05	SW	STEERING WHEEL

TABLE 15  
B.3 CARD INFORMATION WITH NJNT=5

LAST ID	JOINT	JNT	J+1	IPIN
01	W	1	2	2
02	N	1	3	2
03		0	4	0
04	CT	4	5	-4
05	FW	3	6	-4

TABLE 16  
D.2 CARD INFORMATION WITH NPL=5

J	PLTTL(1-5,J)	MNPL(F.1)
1	SEAT BACK	2
2	SEAT CUSHION	1
3	ROOF	1
4	WINDSHIELD	1
5	STEERING WHEEL	3

TABLE 17  
F.1 CARD INFORMATION (8 INTERACTIONS)

LAST ID	NJ	NS(1)	NS(2)	NS(3)
01	1	6	1	1
02	1	6	2	2
03	2	6	2	2
04	3	6	3	3
05	4	6	3	3
06	5	5	1	1
07	5	5	2	2
08	5	5	3	3



**5.3.2 Collision of Two Vehicles with Non-Zero Velocities.** The second model is a collision between two of the man/vehicle systems described in the last subsection. Neither vehicle is accelerating. It is desired to have kinematics relative to the inertial system. Figure 31 illustrates this configuration.

In this case, the vehicles are represented by segments associated with rigid bodies. The primary vehicle is used for an output reference system and is given a zero acceleration profile to keep it coincident with the inertial system. The tables which follow are laid out in a manner similar to the last subsection.

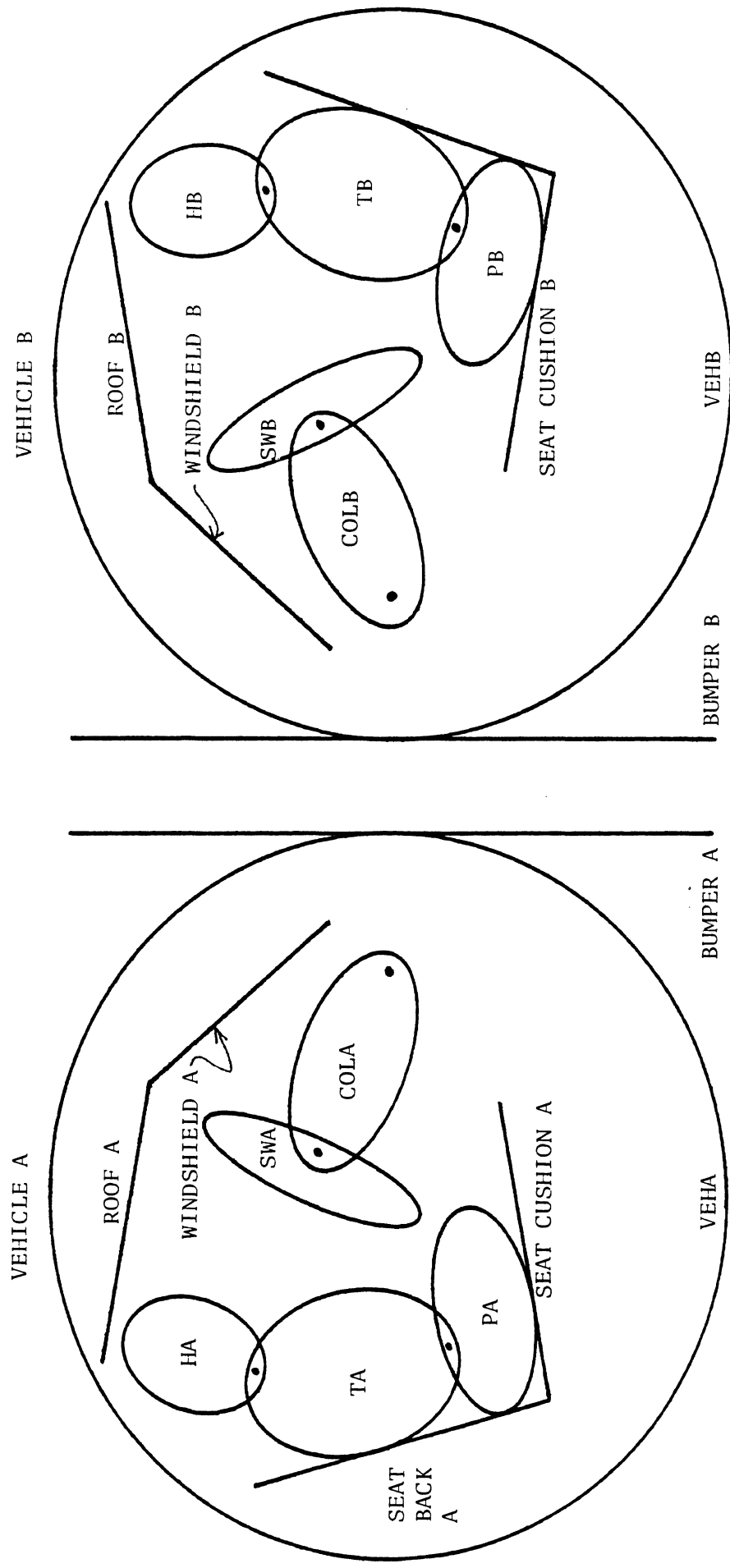


FIGURE 31. Two three-segment vehicles, with three-segment men inside, collide.

TABLE 18

## B.2 CARD INFORMATION WITH NSEG=12

LAST ID	SEG	DESCRIPTION
01	TA	TORSO OF OCCUPANT IN VEHICLE A
02	PA	PELVIS OF OCCUPANT IN VEHICLE A
03	HA	HEAD OF OCCUPANT IN VEHICLE A
04	VEHA	VEHICLE A
05	COLA	STEERING COLUMN IN VEHICLE A
06	SWA	STEERING WHEEL IN VEHICLE A
07	TB	TORSO OF OCCUPANT IN VEHICLE B
08	PB	PELVIS OF OCCUPANT IN VEHICLE B
09	HB	HEAD OF OCCUPANT IN VEHICLE B
10	VEHB	VEHICLE B
11	COLB	STEERING COLUMN IN VEHICLE B
12	SWB	STEERING WHEEL IN VEHICLE B

TABLE 19

## B.3 CARD INFORMATION WITH NJNT=11

LAST ID	JOINT	JNT	J+1	IPIN
01	WA	1	2	2
02	NA	2	3	2
03		3	4	0
04	FWA	4	5	-4
05	CTA	5	6	-4
06		0	7	0
07	WB	7	8	2
08	NB	8	9	2
09		0	10	0
10	FWB	10	11	-4
11	CTB	11	12	-4

TABLE 20

## D.2 CARD INFORMATION WITH NPL=12

J	PLTTL(1-5,J)	MNPL(F.1)
1	SEAT BACK A	2
2	SEAT CUSHION A	1
3	ROOF A	1
4	WINDSHIELD A	1
5	STEERING WHEEL A	3
6	BUMPER A	1
7	SEAT BACK B	2
8	SEAT CUSHION B	1
9	ROOF B	1
10	WINDSHIELD B	1
11	STEERING WHEEL B	3
12	BUMPER B	1

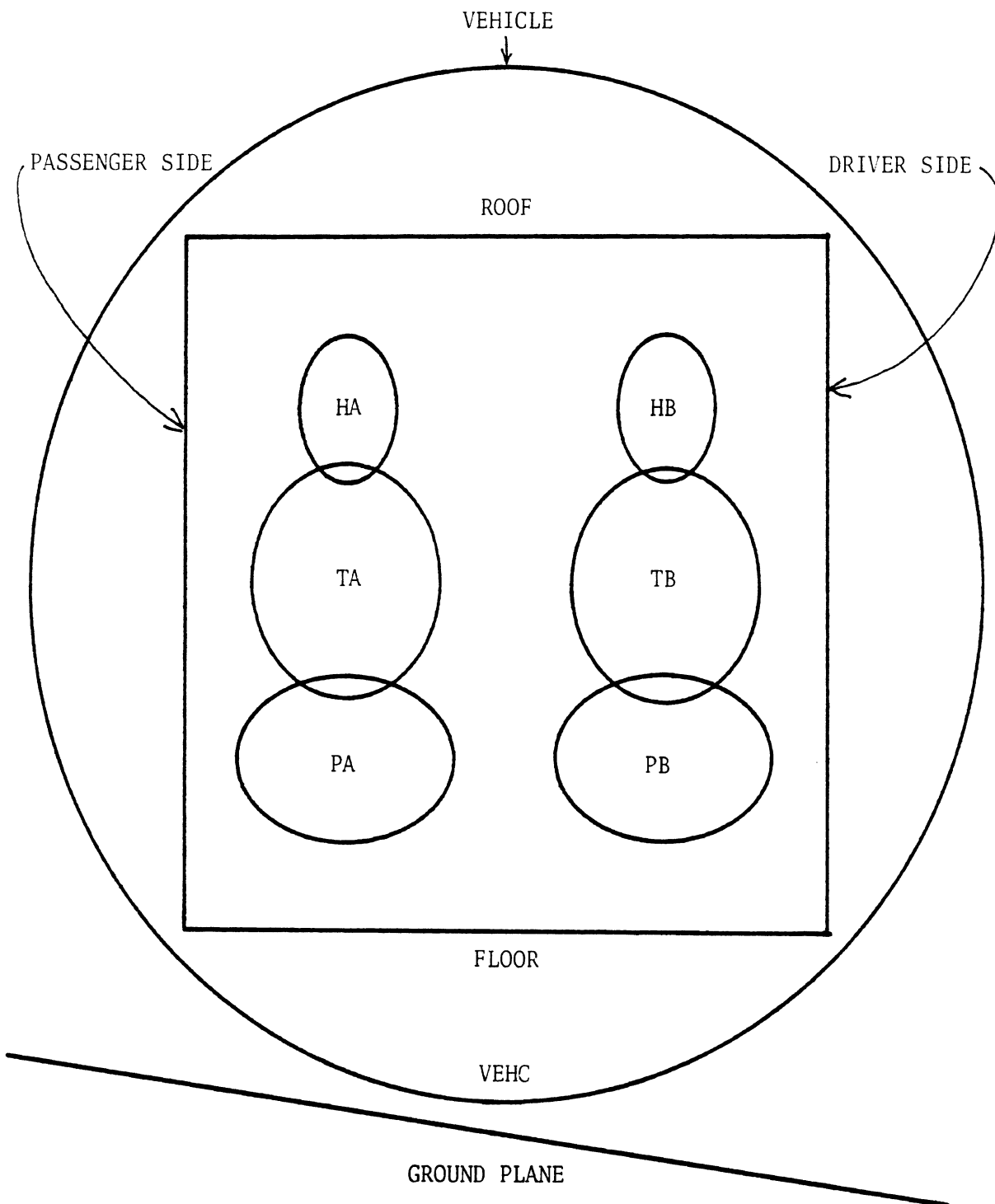
TABLE 21

## F.1 CARD INFORMATION (18 INTERACTIONS)

LAST ID	NJ	NS(1)	NS(2)	NS(3)
01	1	4	1	1
02	1	4	2	2
03	2	4	2	2
04	3	4	3	3
05	4	4	3	3
06	5	6	1	1
07	5	6	2	2
08	5	6	3	3
09	6	4	10	10
10	7	10	7	7
11	7	10	8	8
12	8	10	8	8
13	9	10	9	9
14	10	10	9	9
15	11	12	7	7
16	11	12	8	8
17	11	12	9	9
18	12	10	4	4

**5.3.3 Rollover of Vehicle with Two Occupants.** The third situation has two occupants in one vehicle rolling and bouncing down a hillside. Inertial kinematics are desired. Interest is in occupant interactions with each other and in whether they remain confined in the vehicle. Figure 32 illustrates this configuration.

For this case, the vehicle is again represented by a separate mass. The primary vehicle is again used with a zero acceleration profile to provide a practical output reference frame. The vehicle passenger compartment is represented simply by six interior panels because of the extraordinarily large number of important interactions which can occur even in this simplified case. Each occupant is represented by three segments. The following tables are similar to preceding subsections except that one additional table summarizes the ellipsoid-ellipsoid interaction specifications.



(View from front)

FIGURE 32. Two occupants in vehicle rollover.

TABLE 22

## B.2 CARD INFORMATION WITH NSEG=6

LAST ID	SEG	DESCRIPTION	MNSEG(F.3)
01	TA	TORSO OF OCCUPANT A	3
02	PA	PELVIS OF OCCUPANT A	3
03	HA	HEAD OF OCCUPANT A	3
04	TB	TORSO OF OCCUPANT B	0
05	PB	PELVIS OF OCCUPANT B	0
06	HB	HEAD OF OCCUPANT B	0
07	VEH	VEHICLE	0

TABLE 23

## B.3 CARD INFORMATION WITH NJNT=6

LAST ID	JOINT	JNT	J+1	IPIN
01	WA	1	2	2
02	NA	1	3	2
03		0	4	0
04	WB	4	5	2
05	NB	4	6	2
06		0	7	0

TABLE 24

D.2 CARD INFORMATION WITH NPL=7

J	PLTTL(1-5,J)	MNPL(F.1)
1	ROOF	6
2	PASSENGER DOOR	6
3	FLOOR	6
4	DRIVER DOOR	6
5	FRONT	6
6	BACK	6
7	GROUND PLANE	1

TABLE 25

F.3 CARD INFORMATION (9 INTERACTIONS)

LAST ID	NJ	NH(1)	NS(2)	NS(3)
01	1	1	4	4
02	1	1	5	5
03	1	1	6	6
04	2	2	4	4
05	2	2	5	5
06	2	2	6	6
07	3	3	4	4
08	3	3	5	5
09	3	3	6	6



**5.3.4 Segment Rolling Over Surface of Another Segment.** This last example explores the use of a roll-slide constraint to represent a moving attachment point on the pelvis. The same basic setup is employed as in the first example except the steering wheel and column are left out and, instead, vehicle interior panels are used. One additional small mass, called the roller, is added to roll on the pelvis. This could be used in a simulation of belt migration over the pelvis as would be the case in submarining. Kinematics are with respect to the vehicle and a regular acceleration profile is used to drive the simulation.

Figure 33 illustrates this configuration and the tables are laid out as in preceding sections.

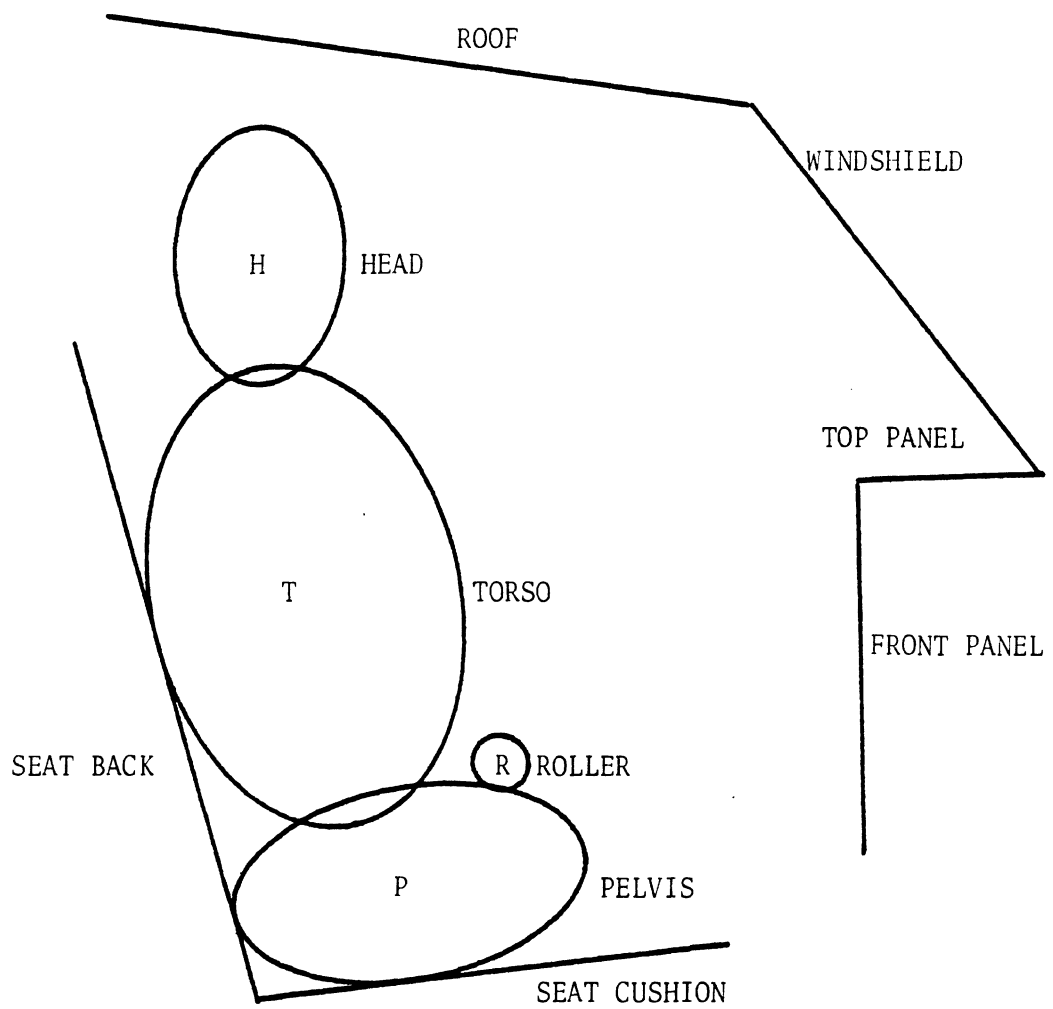


FIGURE 33. Rolling segment on pelvis of occupant in vehicle.

TABLE 26

## F.1 CARD INFORMATION (37 INTERACTIONS)

LAST ID	NJ	NS(1)	NS(2)	NS(3)
01	1	7	1	1
02	1	7	2	2
03	1	7	3	3
04	1	7	4	4
05	1	7	5	5
06	1	7	6	6
07	2	7	1	1
08	2	7	2	2
09	2	7	3	3
10	2	7	4	4
11	2	7	5	5
12	2	7	6	6
13	3	7	1	1
14	3	7	2	2
15	3	7	3	3
16	3	7	4	4
17	3	7	5	5
18	3	7	6	6
19	4	7	1	1
20	4	7	2	2
21	4	7	3	3
22	4	7	4	4
23	4	7	5	5
24	4	7	6	6
25	5	7	1	1
26	5	7	2	2
27	5	7	3	3
28	5	7	4	4
29	5	7	5	5
30	5	7	6	6
31	6	7	1	1
32	6	7	2	2
33	6	7	3	3
34	6	7	4	4
35	6	7	5	5
36	6	7	6	6
37	7	9	7	7

TABLE 27

B.2 CARD INFORMATION WITH NSEG = 4

LAST ID	SEG	DESCRIPTION	MNSEG(F.3)
01	T	TORSO OF OCCUPANT	0
02	P	PELVIS OF OCCUPANT	1
03	H	HEAD OF OCCUPANT	0
04	R	ROLLER	0

TABLE 28

B.3 CARD INFORMATION WITH NJNT = 3

LAST ID	JOINT	JNT	J+1	IPIN
01	W	1	2	2
02	N	1	3	2
03		0	4	0

TABLE 29

D.2 CARD INFORMATION WITH NPL = 6

J	PLTTL(1-5,J)	MNPL(F.1)
1	SEAT BACK	2
2	SEAT CUSHION	1
3	ROOF	1
4	WINDSHIELD	2
5	DASH TOP	2
6	DASH FRONT	2

TABLE 30

## F.3 CARD INFORMATION (1 INTERACTION)

LAST ID	NJ	NS(1)	NS(2)	NS(3)
01	2	2	4	4

TABLE 31

## F.1 CARD INFORMATION (10 INTERACTIONS)

LAST ID	NJ	NH(1)	NS(2)	NS(3)
01	1	5	1	1
02	1	5	2	2
03	2	5	2	2
04	3	5	3	3
05	4	5	1	1
06	4	5	3	3
07	5	5	1	1
08	5	5	3	3
09	6	5	1	1
10	6	5	2	2

## 6.0 THREE-DIMENSIONAL NECK MODELING CONCEPTS

One of the goals of this project was development of a three-dimensional biomechanical neck model. The motivation for this was activity of several researchers during the 1983-1984 period. These included:

- Wismans and Spenny (6) who developed representations of head-neck response in frontal flexion
- Bowman et al. (7) who were doing preliminary two- and three-dimensional simulations of head motion with respect to the torso
- Alem et al. (8), who were obtaining biomechanical data describing the head and neck response to axial impacts
- Goldsmith, Deng, and Merrill (9) who developed a sophisticated three-dimensional head-neck model including effects of individual vertebrae and muscles. In each case, the conclusion was reached that the results were preliminary and that further research was needed. In addition, the biomechanical data bases were different for each group, with the exception of the first two, and the human data were obtained at very low G-levels. As a result, little work was done toward this goal because of the very large amount of time that would be required to synthesize the results of the above researchers into a biomechanically sound model and the small range of applicability that such a model would have. Several GMCVS modeling concepts have been posed in this section that could be used in future efforts.

Figure 34 shows schematic views of three modeling concepts that could be implemented in GMCVS. The first of these models the neck as a rigid link connecting the head to the torso. This model is currently used in most simulations of Hybrid III response. It would be rather easy to adapt the NBDL data to support this concept. However, the humanlike response would be limited to low G-level inputs and sub-injury response levels.

The second model is more sophisticated as it allows for stretching of the neck. The model consists of a tension element connecting the head to the torso and an ellipsoid attached to the torso to resist the downward motion of the head toward the torso. This model could be used to simulate a vertical impact. The data gathered by Alem et al. (8) could be used to define parameters. A shortcoming of this concept is the lack of torsional resistance to head motion with respect to the torso. This shortcoming can be overcome through the use of the new ATB Version 4.0 (soon to be released by the Armstrong Aerospace Medical Research Laboratory). The new sliding joint feature will apparently allow torsional resistance between segments and linear mobility of the joint location.

The third model is even more sophisticated and could be generalized to model the human or Hybrid III linkage. In this case, the flexible element approach is used to kinematically simulate neck extension/compression and both linear and rotational motions of the head with respect to the torso. Two recent ATB developments point toward even more detailed models. The first of these is use of the sliding joint feature mentioned above. This feature could be used to represent compressibility of the disc material separating the

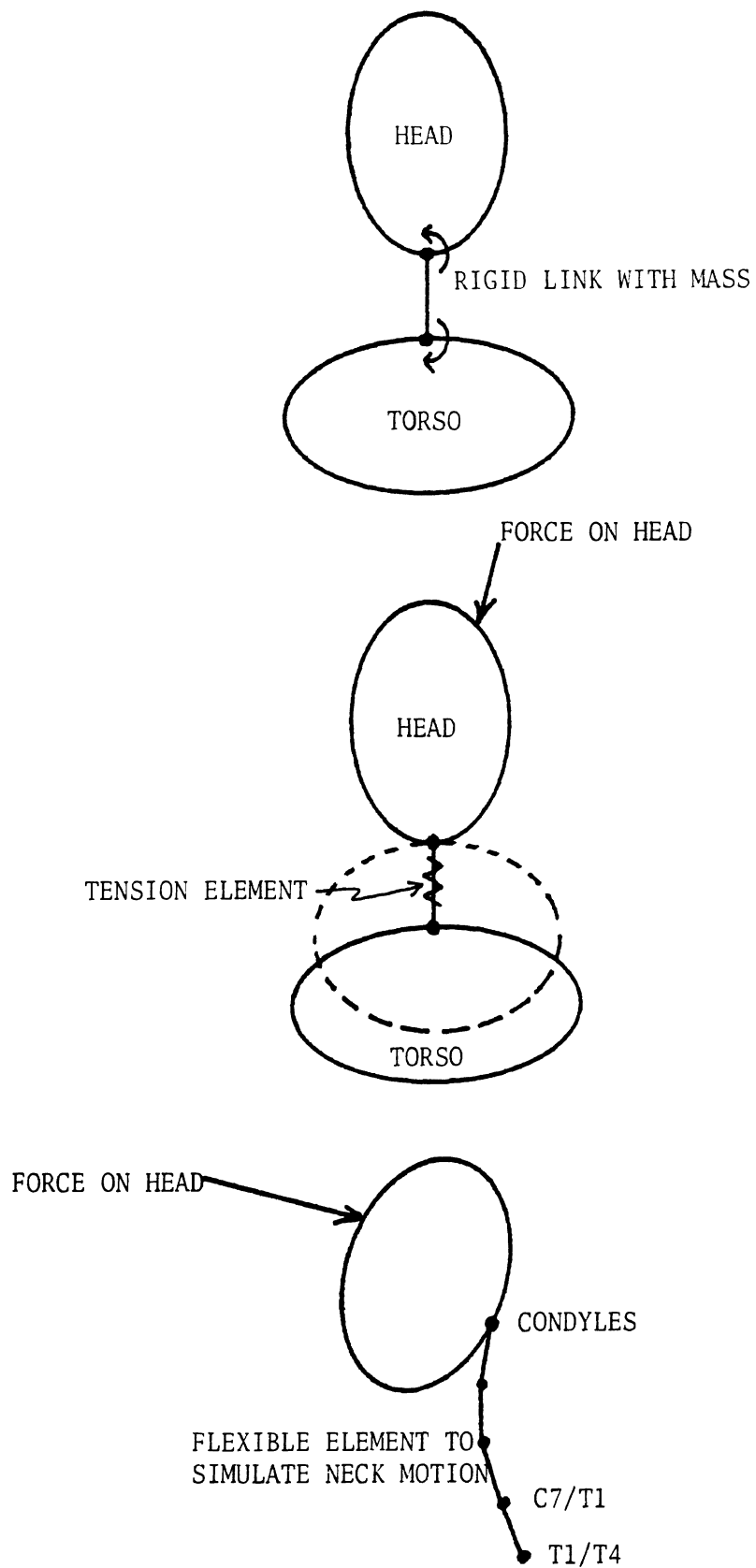


FIGURE 34. Humanlike neck model concepts.

individual vertebrae. The second is addition of active neuromusculature through use of harness elements between the individual body segments (14).

Although the original goal was not reached, it appears that it is now possible to develop advanced three-dimensional neck models due to recent software improvements. This may be particularly useful for simulations of crash test dummy kinematics. However, the problem of range of applicability of human models to low, sub-injury G-levels remains.



## 7.0 SUMMARY OF RESULTS, CONCLUSIONS, AND RECOMMENDATIONS

The following list of items summarizes project findings.

1. The primary goal of this project, development of a rollover simulation capability using three-dimensional crash victim simulation software compatible with that already installed at General Motors (GMCVS), was accomplished.

2. The goal of developing a humanlike three-dimensional analytical neck model was postponed until the biomechanical data base defining three-dimensional neck motion is more established.

3. The capabilities of GMCVS were demonstrated to be applicable to rollovers by use of a simple model consisting of two impacting vehicles, one of which contains a three mass occupant and has a prescribed roll velocity. This model, which also allows the two vehicles to interact with each other, and with the ground, points to a large variety of potential applications including simulation of two occupants in a vehicle.

4. An initial full-scale simulation of a dolly drop test has been made that demonstrates the capabilities of the GMCVS for modeling complex rollover events. Occupant kinematics in the full-scale simulation were qualitatively similar to those obtained from a review of films taken of the original dolly drop rollover test. Also, the results were superior to those generated by the previous MVMA 2-D simulations because of the relaxation of the restraint on vertical knee motion.

5. Guidelines for the layout of GMCVS segment data have been developed. These guidelines provide methods for the user that deal with the general problems of specifying segments and linkages of segments in terms of input to the GMCVS model. The four examples that are given include:

- vehicle crash with occupant, column mass, and wheel mass
- collision of two vehicles with non-zero velocities
- rollover of vehicle with two occupants
- segment rolling over the surface of another segment

These additional items supplement the item describing the full-scale simulation:

1. A primary criterion for the selection of appropriate contact interactions between the occupant and the vehicle is to initially choose those that appear to be the most critical to overall containment of the occupant in the vehicle (unless ejection is the subject of the simulation).

2. Great care must be taken in setting up vehicle motion input due to spline-fit code sensitivity to the shape of the position versus time curves in the neighborhood of time = 0 milliseconds.

3. Rapid oscillatory motions were observed for light weight masses, particularly the hands. This phenomenon can lead to solution instability. The proposed solutions are

addition of damping to the joints used in the Hybrid III data set or elimination of the hand masses from the model.

These final additional items supplement preliminary activity toward the goal of a humanlike three-dimensional analytical neck model.

1. In attempting development of three-dimensional neck models for GMCVS, a review of the biomechanical data base was conducted. Little work was done beyond this because of the very large amount of time that would be required to synthesize the contents of the data base into a biomechanically sound model and the small range of applicability such a model would have due to the low G-loadings developed during human experiments.

2. Three neck modeling concepts were proposed. The most sophisticated of these recommends extension of the GMCVS flexible element approach to include compressibility of disc material using the new ATB slip joints and active neuromusculature. This is accomplished by use of harness elements between individual body segments.

## 8.0 REFERENCES

1. Robbins, D.H. *Three-dimensional Occupant Dynamics Software: Steering Assembly Model*, Report no. UMTRI-85-44, University of Michigan Transportation Research Institute, October 1985, 91 p.
2. Robbins, D.H. and Bennett, R.O. *Three-Dimensional Occupant Dynamics Software: Belt Model Use*, Report no. UMTRI-85-45, University of Michigan Transportation Research Institute, August 1986, 153 p.
3. Lehman, R.J., Bennett, R.O., and Robbins, D.H. *Ellipsoidal Man Plotting Package for MVMA 2-D and CVS (HSRI Version) Occupant Motion Models*, Report no. UMTRI-83-27, University of Michigan Transportation Research Institute, June 1983, 49 p.
4. Robbins, D.H. *Simulation of Occupant Kinematics in Rollovers using the MVMA 2-D Model*, Report UMTRI-83-33, University of Michigan Transportation Research Institute, July 1983, 53 p.
5. Robbins, D.H. and Viano, D.C. *MVMA 2-D Modeling of Occupant Kinematics in Rollovers*, Paper 840860, Society of Automotive Engineers, Warrendale, Pa., May 1984, 13 p.
6. Wismans, J. and Spennney, C.H. "Head-Neck Response in Frontal Flexion," *Proc. 28th Stapp Car Crash Conference*, Society of Automotive Engineers, Warrendale, Pa., November 1984, pp. 161-172.
7. Bowman, B.M., Schneider, L.W., Lustick, L.S., Anderson, W.R., and Thomas, D.J. "Simulation Analysis of Head and Neck Dynamic Response," *Proc. 28th Stapp Car Crash Conference*, Society of Automotive Engineers, Warrendale, Pa., November 1984, pp. 173-206.
8. Alem, N.M., Nusholtz, G.S., and Melvin, J.W. "Head and Neck Response to Axial Impacts," *Proc. 28th Stapp Car Crash Conference*, Society of Automotive Engineers, Warrendale, Pa., November 1984, pp. 275-288.
9. Goldsmith, W., Deng, Y.C., and Merrill, T.H., *Numerical Evaluation of the Three-Dimensional Response of a Human Head-Neck Model to Dynamic Loading*, Paper no. 840861, Society of Automotive Engineers, Warrendale, Pa., May 1984, pp. 79-98.
10. Robbins, D.H., Becker, J.M., Bennett, R.O., and Bowman, B.M. *Accident Data Simulation. Pedestrian and Side Impact-3D*, Report no. UM-HSRI-80-75. University of Michigan Transportation Research Institute, December 1980, 82 p.
11. Padgaonkar, A.J. and Prasad, P. "Simulation of Side Impact Using the CAL3D Occupant Simulation Model," *Proc. 23rd Stapp Car Crash Conference*, November 1979, pp. 133-158.

12. Kaleps, I., Obergefell, L.A., and Ryerson, J.R. *Simulation of Restrained Occupant Dynamics During Vehicle Rollover*, Report DOT-HS-807049, Armstrong Aerospace Medical Research Laboratory, Wright-Patterson AFB, Ohio, June 1986, 97 p.

13. Obergefell, L.A., Kaleps, I., and Johnson, A.K., "Prediction of an Occupant's Motion During Rollover Crashes," *Proc. 30th Stapp Car Crash Conference*, October 1986, pp. 13-26.

14. Freivalds, A. and Kaleps, I. "Modeling of Neuromusculature Response to Dynamic Mechanical Stresses," *1983 Annual Industrial Engineering Conference Proceedings*, Institute of Industrial Engineers, pp. 191-198.